



# Description of phase equilibrium and volumetric properties for CO<sub>2</sub>+water and CO<sub>2</sub>+ethanol using the CPA equation of state

M.F. Monteiro\*, M.H. Moura-Neto, C.G. Pereira, O. Chiavone-Filho

Departamento de Engenharia Química, Universidade Federal do Rio Grande do Norte - UFRN, Campus Universitário, Lagoa Nova, Natal, Rio Grande do Norte, 59066-800, Brazil

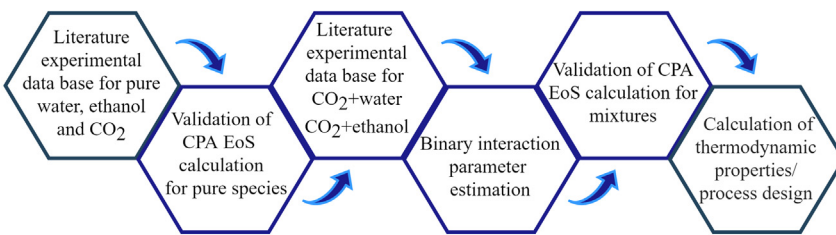


## HIGHLIGHTS

- Literature experimental data on phase behavior and density for water, ethanol and CO<sub>2</sub>.
- Literature data bank on phase equilibrium and density for CO<sub>2</sub>+water and CO<sub>2</sub>+ethanol.
- Data selected for wide ranges of T, P and composition and kij estimation for CPA EoS.
- Application of CPA EoS with CR-1 for phase equilibrium and volumetric description.
- Validation of CPA EoS for calculation of thermodynamic properties and process design.

## GRAPHICAL ABSTRACT

### Phase Equilibrium and density description



## ARTICLE INFO

### Article history:

Received 16 December 2019  
Received in revised form 16 March 2020  
Accepted 17 March 2020  
Available online 19 March 2020

### Keywords:

Phase equilibria  
Density  
High pressure  
Cubic plus association  
Thermodynamic calculation

## ABSTRACT

Properties of fluids under high pressure is of interest for processes design. A literature survey was conducted on experimental vapor-liquid equilibrium (VLE) and density for CO<sub>2</sub>+water and CO<sub>2</sub>+ethanol. Phase equilibrium and density of pure water, ethanol and CO<sub>2</sub> were evaluated considering 1868 data points. VLE and saturated liquid density data were collected: 544 data points for CO<sub>2</sub>+water and 859 data points for CO<sub>2</sub>+ethanol. Soave Redlich-Kwong (SRK) equation of state (EoS) with Cubic Plus Association (CPA) was applied for calculation of these properties. Peng-Robinson EoS was evaluated to demonstrate CPA improvement in properties description. The binary interaction parameters were estimated from VLE. For pure compounds, the results indicated suitable description for both phase behavior and density. For CO<sub>2</sub>+water, density calculations were accurate ( $\Delta\rho=0.5\%$ ) and VLE was adequately described ( $\Delta x_{H2O}=0.49\%$  and  $\Delta y_{CO2}=4.63\%$ ). CO<sub>2</sub>+ethanol volumetric behavior and VLE were also satisfactorily described in CO<sub>2</sub> concentrations up to 30% ( $\Delta\rho=2.92\%$ ,  $\Delta x_{EtOH}=1.37\%$  and  $\Delta y_{CO2}=5.86\%$ , respectively).

© 2020 Elsevier B.V. All rights reserved.

## 1. Introduction

Nowadays, studies involving solvents and mixtures of solvents at high pressures have important industrial applications. Many sep-

aration processes e.g. distillation and absorption are conducted at high pressure to ensure economic feasibility. The study of CO<sub>2</sub>+water system, for instance, is useful to represent pre salt reservoir conditions due to the large amounts of CO<sub>2</sub> present up to 20% [1]. This application endorses the study of pressures around 100 MPa and temperatures up to 473 K [2]. Thereby, understanding phase behavior of this system is important for design of oil and gas exploitation process [3]. CO<sub>2</sub> sequestration and geological stor-

\* Corresponding author.

E-mail address: [mateus@nupeg.ufrn.br](mailto:mateus@nupeg.ufrn.br) (M.F. Monteiro).

age is another operation that justifies the study in a wide pressure range. And not only in these sectors, in the food and pharmaceutical, it is observed alcohols as co-solvents for CO<sub>2</sub> in high pressure extraction of biomaterials from herbs [4]. The same process is also highly used in the extraction of ingredients, such as flavor and colorants, from plants and fruits by the food and cosmetics industry [5].

In this context, it has been observed the higher application of some solvents in particular, such as carbon dioxide, ethanol and water. Carbon dioxide (CO<sub>2</sub>) is the most widely used supercritical solvent because of its mild critical conditions (304.25 K and 7.383 MPa) and low costs. Furthermore, low toxicity and non-flammable properties contribute for CO<sub>2</sub> uses. However, the solvation of polar compounds by CO<sub>2</sub> is limited. It may be improved by the addition of polar miscible compounds, usually called co-solvent or modifier [6], which provide the increase of the solute solubility in supercritical fluids due to physical and chemical interactions between co-solvent and solute [7]. Among the green solvents, ethanol and water have demonstrated good results as a modifier in process at higher pressures [8–12].

CO<sub>2</sub>+water mixture present type III phase behavior [13–15] while CO<sub>2</sub>+ethanol type I. [16–18] in the classification of Scott and van Konynenburg [19,20]. The type III mixtures present two discontinuous critical lines: a small vapor-liquid and a fluid-fluid. The critical line extending from gas-liquid critical point of the more volatile component ends at an upper critical end point where the gaseous phase and the liquid phase have the same compositions. Type I systems are characterized by the presence of a continuous gas-liquid critical line and absence of liquid-liquid immiscibility [21].

Thermodynamic models are widely applied to describe equilibrium and volumetric properties for process design, simulation and operation. For high pressure processes e.g. supercritical fluid extraction and adsorption, Equations of State (EoSs) are models usually applied to describe the phase behavior. It is crucial to ensure that the properties of pure fluids and mixtures are being estimated appropriately. Thereby, an extensive validation of the EoS against experimental data is required before application.

The study of the properties of pure water, ethanol and CO<sub>2</sub>, as well as the CO<sub>2</sub>+ethanol and CO<sub>2</sub>+water systems is of great importance for technology development. The applications presented for these two binary systems in various industrial areas require high accuracy calculation methods for the phase behavior and volumetric properties. For instance, the evaluation and optimization of the processes involved in oil production, CO<sub>2</sub> sequestration and geological storage, pharmaceutical area and food processing are feasible.

Kontogeorgis et al. [22] developed Cubic Plus Association (CPA) EoS. In this equation there are five pure compound parameters, estimated from vapor pressure and liquid density data. Applications of the CPA EoS to calculate properties of normal chain alcohols and water were also presented, and it was demonstrated accurate representation of vapor pressures and liquid densities for a series of species.

The first CPA application for mixtures was presented by Yakkoumis et al. [23]. CPA EoS performance was evaluated for binary aqueous mixtures containing alkanes, cycloalkanes and alkenes. Three different association schemes for the water molecule were applied in the correlation of liquid-liquid equilibrium data, i.e.: 2B, 3B and 4C, using Huang and Radosz notation [24]. Among them, 4C association scheme is clearly superior to the others. This association scheme describes two donor and two electron receptor sites, capable of forming 4 hydrogen bonds with neighboring molecules. Average deviations between 5 and 15% in water mole fraction in hydrocarbon-rich phase were reported for the CPA EoS. It was also demonstrated that CPA presented better results than SAFT (Statistical Associating Fluid Theory) [25]. Nowadays, CPA EoS is

a consolidate model and it is available in commercial simulation softwares, e.g., PetroSIM™ and Aspen-Hysys.

A satisfactory representation of CO<sub>2</sub> in mixtures with other polar molecules could not be obtained with CPA EoS by treating it as a non-associated molecule [26,27]. This is because CPA does not explicitly account for the weak quadrupolar interactions that occur in the carbon dioxide molecule. Average deviations in vapor pressure suggest that the non-associated scheme reflects in errors four times greater when compared to the results obtained with associated schemes. For liquid density, these errors get up to 8 times greater. However, the use of CPA EoS neglecting the CO<sub>2</sub> association was still applied in the literature [28].

Classical EoSs are widely available in commercial softwares, e.g., PRO-II and ProSim Plus contributing for their extensive use. Furthermore, the simplicity of cubic EoS contributes for industrial applications [29]. CO<sub>2</sub>+water modeling has been extensively explored in literature using classical equations of state with fitted interaction parameters. Fenghour et al. [30] successfully described the density and dew points of this mixture using Peng-Robinson (PR) EoS at 415–700 K and 35 MPa. Hou et al. [31] experimentally studied the phase behavior of CO<sub>2</sub>+water at 298.15–448.15 K and 1.5–18 MPa. Gamma-phi approach was applied using PR EoS with classical mixing rules for vapor phase and an extended form of Henry's law with NRTL (Non-Random Two Liquids) solution model together with a Poynting correction for the liquid phase. These authors also compared their approach against literature experimental data and found satisfactory results. Phase behavior of systems containing water and supercritical fluids, e.g., H<sub>2</sub> [32] and CO<sub>2</sub> [33] were successfully described applying PR78 EoS [34]. Qian et al. [35] applied a group contribution method into PR78 EoS for binary aqueous systems containing hydrocarbons and gases. An extensive data base of experimental bubble points (P,T,x), dew points (P,T,y) and binary critical points for CO<sub>2</sub>+water was built. High accuracy was reported for phase behavior modeling with one interaction parameter adjusted for each isotherm.

The associative term presented by Kontogeorgis et al. [22] has also been explored for CO<sub>2</sub>+water description. Pappa and co-workers [36] determined VLE data for CO<sub>2</sub>+water mixture at 383–623 K and pressure up to 140 MPa, and obtained suitable results in its behavior description using the PR equation + association term considering 4C association scheme for CO<sub>2</sub> ( $\Delta x_{\text{CO}_2} = 5.9\%$  and  $\Delta y_{\text{H}_2\text{O}} = 9.6\%$ ). SRK-CPA, PR-CPA and PC-SAFT were evaluated for pure water and CO<sub>2</sub>+water modeling [37]. Different association schemes for water (2B, 3B, 4C) were applied. Although the three equations showed adequate results for the phase behavior description, PC-SAFT was the most accurate.

More recently, Aasen [38] used CPA with CO<sub>2</sub> as a non-associated molecule and one binary interaction parameter to describe density and VLE of CO<sub>2</sub>+water. The influence of carbon dioxide association scheme on pure CO<sub>2</sub> and CO<sub>2</sub>+water systems modeling was also studied. The non-associated and 2B, 3B, 4C association schemes were evaluated, and concluded that the 4C scheme presented the best CO<sub>2</sub> representation. Beside the original method, Tsivintzelis et al. [28] also proposed a second approach that used experimental data to obtain the association energy parameter instead of applying combining rule 1 (CR1), with adjustable interaction parameter. This approach satisfactorily described VLE data. Perfetti [39] used the CPAMSA (Mean Spherical Approximation) to correlate literature VLE data and obtained 5% mean error in liquid composition. The CPAMSA presented six adjustable parameters and it was significantly more complex due to a specific term to account for dipolar interactions.

Hadi [40] and Kariznovi et al. [41] compared PR and Soave Redlich-Kwong (SRK) EoSs in the description of phase equilibrium of CO<sub>2</sub>+ethanol at 288–323 K and pressure up to 1.9 MPa. The former evaluated 3 mixing rules in the description of liquid and vapor

compositions, and observed that the best results were obtained for the mixing rule MR3, with 2 adjustable parameters. The latter indicated satisfactory results for liquid compositions and densities for both EoSs. PR equation with two fitted interaction parameters was evaluated by Stievano and Elvassore [42] for the correlation of VLE and density data of the same system at 291.15–323.15 K and pressure up to 18 MPa. A satisfactory description of both volumetric and equilibrium properties was not obtained. These authors also used a modification of original SAFT proposed by Huang and Radosz [43], which presented better results than PR EoS ( $\Delta P = 1.05\%$  and  $\Delta \rho = 1.025\%$ ). Chienming et al. [44] compared Patel-Teja (PT) and PR EoS in the representation of phase equilibria of CO<sub>2</sub>+ethanol. The average deviations between experimental and correlated data in this study were less than 4%, indicating that both EoSs are applicable for these VLE. However, better results were obtained with PT EoS ( $\Delta P = 2.9\%$  and  $\Delta y_{\text{EtOH}} = 0.26\%$ ). Patel-Teja with an empirical density-dependent local composition mixing rule was applied for description of CO<sub>2</sub>+ethanol phase behavior [45]. It was demonstrated a satisfactory description due to the sophisticated mixing rule applied.

CPA EoS was evaluated by Oliveira et al. [46] for the description of CO<sub>2</sub>+ethanol phase behavior at 291.1–313.14 K and 1–30 MPa. The 2B and 4C association schemes for CO<sub>2</sub> were applied. Considering CO<sub>2</sub> as non-associating and interaction parameter ( $k_{ij}$ ) independent of temperature ( $T$ ) was obtained ( $\Delta x_{\text{CO}_2} = 15.3\%$  and  $\Delta y_{\text{CO}_2} = 2.13\%$ ). Assuming a temperature dependency on  $k_{ij}$  improved liquid phase description ( $\Delta x_{\text{CO}_2} = 8.8\%$ ) and did not affect vapor phase. For liquid densities, deviations up to 5.8% were reported at 291.15 K. Perakis et al. [26] compared SAFT and CPA EoSs to represent VLE of CO<sub>2</sub>+ethanol at 313.4–344.7 K and pressure up to 12 MPa. Calculated values were compared with 31 experimental data points from one source. According to these authors, CPA EoS cannot describe satisfactorily the liquid phase composition considering CO<sub>2</sub> as non-associating ( $\Delta x_{\text{CO}_2} = 9.2\%$  and  $\Delta y_{\text{CO}_2} = 2.6\%$ ). Two combining rules (CR-1 and CR-2) were applied for CPA and significant effect on the model performance was not observed. Volumetric properties were not evaluated.

In this work, extensive phase equilibrium and liquid density data were collected from literature for the systems CO<sub>2</sub>+water and CO<sub>2</sub>+ethanol. In order to describe volumetric properties and VLE behavior of the systems, the original CPA EoS with combining rule 1 was applied, checking its validity in a wide range of temperature, pressure and composition. The main objective was to endorse the use of CPA for the calculation of these properties for the two binary systems and the respective pure components.

## 2. Methodology

Experimental data of vapor pressure ( $P^{\text{vap}}$ ) and liquid density ( $\rho$ ) of pure water ( $P^{\text{vap}} = 275$  data points;  $\rho = 679$  data points), ethanol ( $P^{\text{vap}} = 281$  data points;  $\rho = 353$  data points) and CO<sub>2</sub> ( $P^{\text{vap}} = 146$  data points;  $\rho = 134$  data points) were collected from literature as shown in Table 1.

Complete experimental data of phase equilibrium ( $T$ ,  $P$ ,  $x$ ,  $y$ ) were selected (CO<sub>2</sub>+water: 239 data points; CO<sub>2</sub>+ethanol: 717 data points), allowing a check of thermodynamic consistency. Data selection strategy was based on this consistency check and the agreement between experimental data from different references. Using this criterium various references were not considered in the databank for parameter estimation, mainly PTx and PTy data sets.

Saturated liquid density of CO<sub>2</sub>+water ( $\rho = 305$  data points) and CO<sub>2</sub>+ethanol ( $\rho = 142$  data points) were also collected from literature. Phase behavior and density data are presented in Table 2.

SPECS v5.63 (Separation and Phase Equilibrium Calculations) was used to perform flash calculations using CPA EoS. For

**Table 1**  
Pure component vapor pressure and liquid density data.

	NDP	T ranges (K)	P ranges (MPa)	Ref.
Water $P^{\text{vap}}$	8	412–503	0.3–2.8	[47]
	8	507–570	3.0–8.3	[48]
	6	293–343	0.0024–0.031	[49]
	3	648	21	[50]
	78	273–647	0.00061–21.9	[51]
	15	323–353	0.01–0.4	[52]
	64	361–428	0.06–0.6	[53]
	37	383–646	0.1–21.8	[54]
	35	363–645	0.07–21.6	[55]
	9	423–623	0.4–16.5	[56]
Water Density	12	273–647	0.00061–21.9	[57]
	67	293–338	0.09–904	[58]
	7	633	21–33	[59]
	58	283–348	0.1–207.7	[60]
	120	273–323	0.1–20	[61]
	121	323–773	4.5–193.4	[62]
	306	423–773	0.1–36	[63]
	22	277–319	0.002–0.024	[64]
	74	281–351	0.002–0.1	[65]
	5	278–338	0.002–0.058	[66]
Ethanol $P^{\text{vap}}$	29	423–513	0.9–6.12	[67]
	9	409–501	0.7–6.2	[68]
	17	363–514	0.2–6.3	[69]
	26	360–402	0.2–0.6	[53]
	23	364–513	0.2–6.1	[70]
	12	361–498	0.2–4.7	[71]
	26	141–445	0.8–1.6	[72]
	9	308–348	0.014–0.088	[73]
	8	273–351	0.001–0.1	[74]
	21	333–473	0.05–2.9	[75]
Ethanol Density	44	200–350	1–5	[76]
	218	310–400	0.1–200	[77]
	46	298–323	0.1–310	[78]
	45	298–323	0.1–310	[79]
	9	229–270	0.8–3.2	[80]
	7	273–304	3.4–7.2	[81]
	15	222–305	0.7–7.4	[82]
	18	228–289	0.82–5.1	[83]
	7	216	0.5	[84]
	66	222–302	0.6–6	[85]
CO <sub>2</sub> $P^{\text{vap}}$	10	373	2.5–25.3	[86]
	9	423	2.5–30.4	[87]
	32	293–303	0.1–5.6	[88]
	39	273–423	3.6–125	[89]
CO <sub>2</sub> Density	44	280–320	4.1–31	[90]

CO<sub>2</sub>+water a binary interaction parameter was regressed for each isotherm using isofugacity criteria due to wide temperature range. A quadratic relation between  $k_{ij}$  and temperature was observed. For CO<sub>2</sub>+ethanol one binary interaction parameter ( $k_{ij}$ ) was regressed from VLE data. For this system, binary interaction parameter temperature dependence was neglected due to the small temperature range. The average absolute deviations between the experimental data and the calculated values from EoS CPA were evaluated. CPA pure components parameters were retrieved from literature as reported in Table 3. The CPA parameters were estimated with experimental data ranging from 0.55 to 0.90  $T_r$  (reduced temperature).

For all properties evaluated, the relative deviation between the literature experimental data and the EoS CPA calculated values was defined as:

$$\Delta M = \frac{100}{NDP} \times \sum_{i=1}^{NDP} \left| \frac{M^{i,\text{calc}} - M^{i,\text{exp}}}{M^{i,\text{exp}}} \right| \quad (1)$$

Where  $M$  is the liquid molar fraction, vapor molar fraction or liquid density.  $NDP$  denotes the number of data points. Superscripts *calc* and *exp* stand for calculated and experimental properties, respectively. A verification of critical point of the pure components with

**Table 2**

Vapor-liquid equilibrium ( $T, P, x, y$ ), saturated liquid density and critical locus data of binary mixtures:  $\text{CO}_2$ +water and  $\text{CO}_2$ +ethanol.

	NDP	$T$ range (K)	$P$ range (MPa)	Ref.
$\text{CO}_2$ +Water $P^{\text{vap}}$	8	412 - 503	0.3–2.8	[91]
	12	273 - 647	0.00061–21.9	[57]
	29	323 - 353	4–14	[92]
	20	278 - 318	1–8	[93]
	34	298 - 448	1–17	[94]
	29	541 - 573	30–100	[15]
	7	323	6.8–17.7	[95]
	48	373 - 493	0.8–8.1	[96]
	5	421	10.1–19.7	[97]
	7	308	1.1–8.0	[98]
	40	383 - 543	10–100	[99]
	167	283 - 333	1.1–30.7	[100]
	32	382 - 468	3.5–103.2	[101]
	24	278 - 293	6.4–29.5	[102]
	15	304	1.0–8.0	[103]
$\text{CO}_2$ +Water Density	33	353 - 471	2.0–10.2	[104]
	29	292 - 298	5.6–45.2	[105]
	5	298	8.9–21.2	[106]
	9	563 - 643	23.5–71.6	[15]
	5	543 - 623	32.5–123	[99]
	53	313 - 343	0.5–12	[107]
	43	312 - 373	0.5–14	[108]
	46	293 - 353	0.5–11	[18]
	29	313 - 343	5–12	[109]
	19	304 - 308	3.7–7.7	[110]
$\text{CO}_2$ +Ethanol $P^{\text{vap}}$	30	304 - 323	3.3–8.0	[111]
	24	313 - 333	0.5–10.6	[112]
	23	313 - 333	0.5–10.6	[113]
	23	314 - 337	5.5–10.8	[114]
	18	313 - 323	0.6–8.1	[115]
	19	308	1.5–7.7	[116]
	67	291 - 313	0.9–8.0	[117]
	60	291 - 313	0.9–8.0	[118]
	52	303 - 329	1.8–9.1	[119]
	60	291 - 313	0.9–8.0	[120]
	22	323 - 392	1.3–10.7	[121]
	12	323	5.0–8.2	[122]
	8	333	4.3–9.5	[123]
	11	333 - 353	5.5–12.0	[124]
	7	333	3.0–10.4	[125]
$\text{CO}_2$ +Ethanol Density	9	291	2.1–5.4	[126]
	31	313 - 353	1.3–13.5	[127]
	43	293 - 353	0.5–11.0	[18]
	8	333	4–10	[128]
	12	303 - 323	1.1–6.0	[129]
	10	291	1.1–4.4	[130]
	48	298 - 313	1.1–7.7	[44]
	7	313	2.0–8.1	[131]
	35	291 - 343	0.1–11.2	[132]
	30	313 - 328	0.6–8.9	[133]
$\text{CO}_2$ +Ethanol Critical locus	4	322 - 340	9.4–11.3	[134]
	5	305 - 325	7.6–8.1	[135]
	4	312 - 373	8.1–14.3	[136]
	7	310 - 410	7.7–15.2	[137]
	5	313 - 344	8.1–12.0	[138]
	4	311 - 347	8.1–12.4	[139]
	6	307 - 317	7.5–8.7	[17]
	4	333 - 453	10.8–13.3	[140]
	2	383 - 493	8.9–14.7	[141]
	10	321 - 364	9.1–13.9	[142]
$\text{CO}_2$ +Ethanol Critical locus	4	333 - 453	10.8–13.3	[143]
	19	319 - 507	7.3–15.1	[144]

**Table 3**

CPA EoS pure-components parameters.

	$a_0$ (bar l <sup>2</sup> mol <sup>-2</sup> )	$b$ (l mol <sup>-1</sup> )	$c_1$	$\epsilon^{\text{AB}}$ (bar l mol <sup>-1</sup> )	$\beta^{\text{AB}} \cdot 10^3$	Association Sheme	$T_c$ (K)
Water*	1.228	0.01452	0.6736	166.55	69.2	4C	647.13
Ethanol*	8.6716	0.04908	0.7369	215.32	8.0	2B	513.92
$\text{CO}_2$ **	110.49	0.02841	0.66	42.65	25.7	4C	304.21

\* Kontogeorgis, G.M.; Yakoumis, I.V.; Meijer, E.M.; Moor-Wood, H. [145].

\*\* Bjørner, M. G.; Kontogeorgis, G. M. [146].

**Table 4**

Vapor pressure deviation between experimental and predicted values for pure species.

Compound	P <sup>vap</sup> deviations ( $\Delta P$ , %)		
	CPA EoS	PR EoS*	SRK EoS**
water	0.076	0.22	5.130
ethanol	0.120	1.30	3.123
$\text{CO}_2$	0.330	0.29	0.546

\* Retrieved from Qian et al. (2013) [35].

\*\* Retrieved from Mingjian et al. (2007) [148].

CPA EoS was performed. CPA was also submitted to calculate the studied binary Critical Locus.

### 3. Results and discussion

#### 3.1. Pure components

The first step in our study was to evaluate the application of CPA for vapor pressure and liquid density data for pure components. Fig. 1 shows experimental and predicted bubble temperature for water (Fig. 1A and B), ethanol (Fig. 1C and D) and  $\text{CO}_2$  (Fig. 1E and F).

According to Fig. 1, CPA EoS satisfactorily described the vapor pressure of pure water ( $\Delta T_b = 0.076\%$ ), ethanol ( $\Delta T_b = 0.12\%$ ) and  $\text{CO}_2$  ( $\Delta T_b = 0.33\%$ ) in the complete experimental temperature range. It should be noted that the errors reported for the DIPPR correlation (water: 0.2%; ethanol: 1%;  $\text{CO}_2$ : 1%) were greater than the obtained with CPA EoS. The agreement between CPA calculations and all literature data evaluated for these components was observed. The deviations observed for CPA EoS calculations are close to the reported experimental uncertainties. The agreement between CPA predictions and DIPPR [147] correlations was also verified. For  $\text{CO}_2$ , eight experimental data points presented higher deviations ( $\Delta T_b^{\max} = 0.55\%$ ) when compared with other experimental data points, indicating experimental errors. Comparing the performance of the classical cubic EoSs (PR and SRK), CPA presented an accurate description of vapor pressure, as presented in Table 4.

Figs. 2–4 presents experimental and predicted densities of pure water, ethanol and  $\text{CO}_2$  respectively.

CPA was also applied for density calculations of pure components. For water, the deviation in density ( $\Delta\rho = 1.68\%$ ) increased along temperature and pressure, as seen in Fig. 2A. Fig. 2B demonstrated the accuracy of CPA calculations in a wide temperature range (283–673 K) and for pressures up to 200 MPa. For extremely high pressures deviations between experimental and predicted densities increase ( $\Delta\rho = 3.90\%$  for pressures above 200 MPa at 323 K). However, this error magnitude is still satisfactory for industrial applications. The accuracy of calculations for the region of lower densities was also demonstrated.

Fig. 2C and D presented density deviations as function of temperature and pressure, respectively. Borzunov et al. [58] presented density experimental data points at low temperature for pure water. However, due to extremely high-pressure conditions relatively higher deviations were observed. Tanishita et al. [62] and Kell et al. [63] presented data points at low pressure for the same

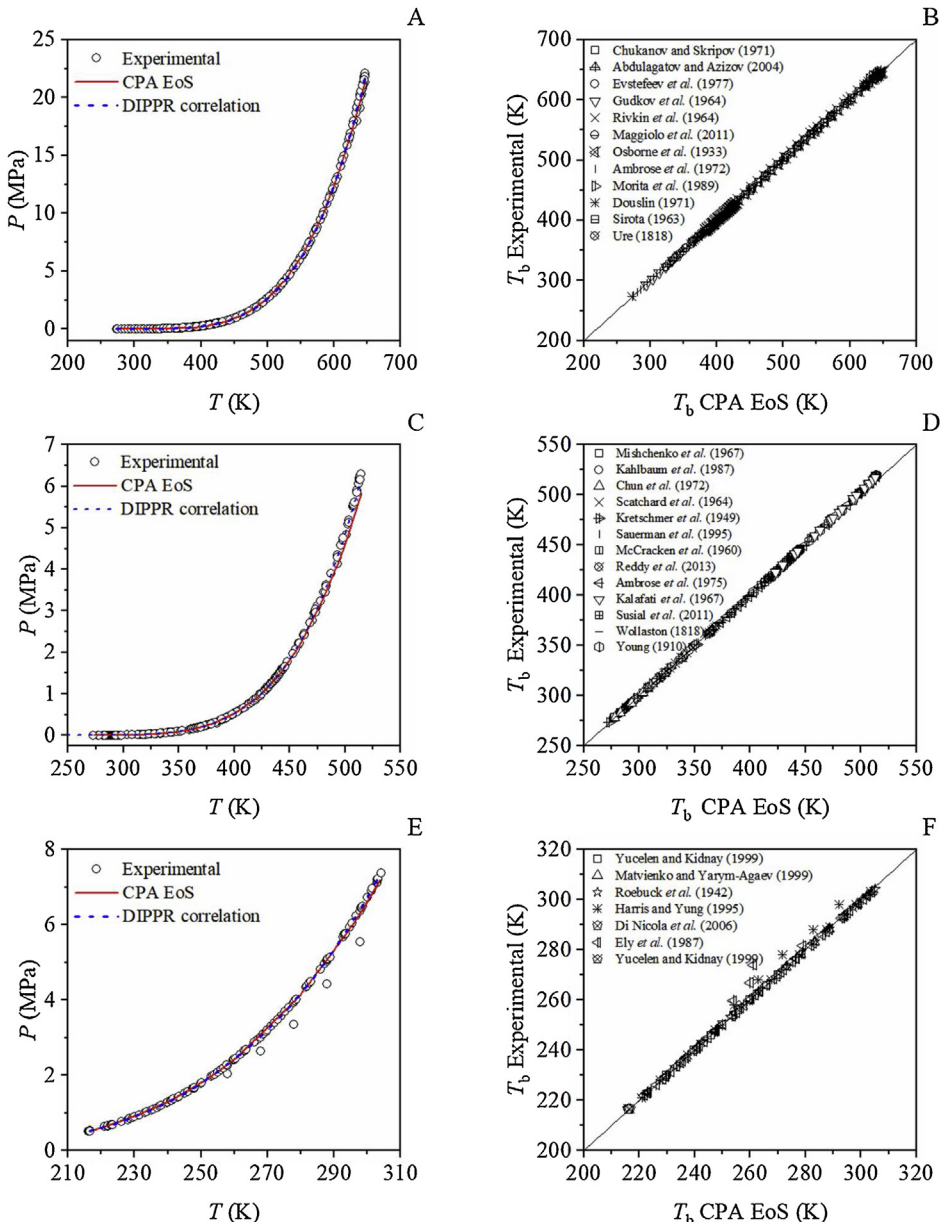


**Fig. 1.** Prediction of bubble temperature of pure compounds using CPA EoS (solid red line), DIPPR correlation [147] (blue dashed line) and experimental data. (A) Water bubble pressure; (B) Comparison of estimated versus experimental bubble temperature for water; (C) Ethanol bubble pressure; (D) Comparison of estimated versus experimental bubble temperature for ethanol; (E)  $\text{CO}_2$  bubble pressure; (F) Comparison of estimated versus experimental bubble temperature for  $\text{CO}_2$ .

component, though relatively higher deviations of CPA EoS were observed due to high temperature experimental conditions. For pressures up to 50 MPa and critical temperature (647.13 K) it was observed an average relative deviation ( $\Delta\rho$ ) of 1.47%.

Experimental and calculated ethanol densities ( $\Delta\rho = 1.59\%$ ) are presented in Fig. 3A. Calculated values were lower than experimental ones for the majority.

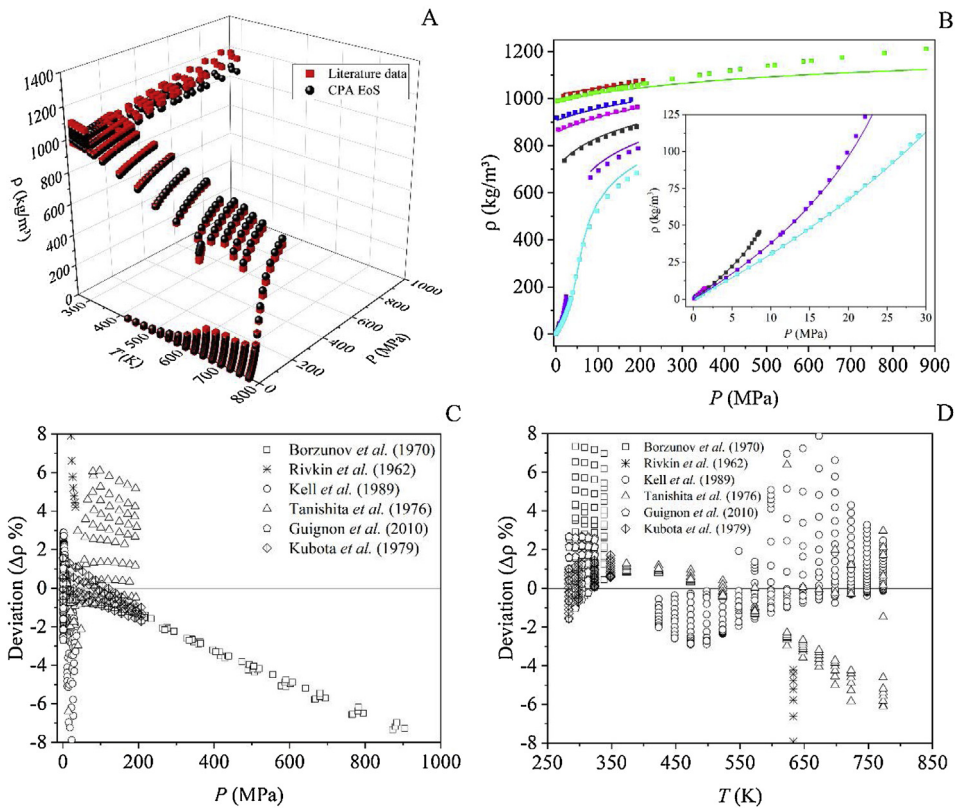
Fig. 3B indicated the accuracy of CPA calculations for ethanol density at pressures up to 50 MPa for the complete temperature range (323–480 K). For pressures above 50 MPa and lower temperatures (up to 380 K) CPA presented significant underestimation (in average 2.6%).

Fig. 3C and D show density deviations as function of pressure and temperature, respectively. Golubev *et al.* [76] presented four isothermal data sets at 200, 250, 300 and 350 K. CPA density deviations for these isotherms were 3.80, 2.24, 1.07 and 0.68%, respectively. For lower temperatures, it was observed higher devi-

tions, as expected due to experimental uncertainties. Takiguchi *et al.* [77] was the only reference which the calculated densities presented positive deviations at temperatures greater than 400 K and low pressures. The EoS calculated densities for the conditions published by Tanaka *et al.* [79] presented higher deviations at elevated pressures. Experimental and calculated  $\text{CO}_2$  densities are presented in Fig. 4A.

According to Fig. 4, carbon dioxide liquid density values calculated by CPA were also adequately described ( $\Delta\rho = 2.44\%$ ). It was observed an inversion in the behavior presented by this equation around 60 MPa. For pressures lower than 60 MPa, CPA EoS calculated smaller values of density in relation to the experimental ones. On the other hand, for greater pressures the opposite behavior was verified. Fig. 4B indicated CPA accuracy in a wide density range.

Fig. 4C and D presented density deviations as function of pressure and temperature, respectively. Data sets presented by Khazanova *et al.* [88] did not agree with other sources. The CPA



**Fig. 2.** Density of pure water. (A) Literature experimental data (red) and calculated from CPA EoS (black) as function of pressure and temperature; (B) Prediction of isothermal density curves (solid lines CPA; ■ experimental data) at seven different temperatures:  $T_1 = 283\text{ K}$  (red),  $T_2 = 323\text{ K}$  (green),  $T_3 = 423\text{ K}$  (blue),  $T_4 = 473\text{ K}$  (pink),  $T_5 = 573\text{ K}$  (grey),  $T_6 = 673\text{ K}$  (violet),  $T_7 = 673\text{ K}$  (cyan); (C) Density relative deviation as function of pressure; (D) Density relative deviation as function of temperature.

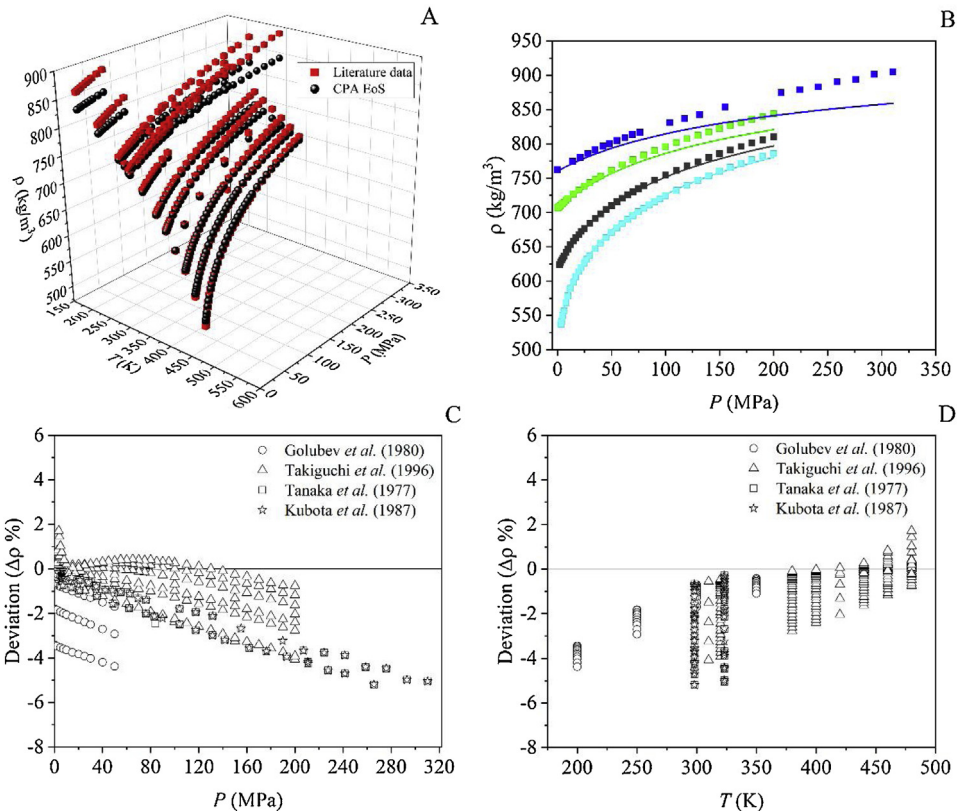


**Fig. 3.** Density of pure ethanol. (A) Literature experimental data (red) and calculated from CPA EoS (black) as function of pressure and temperature; (B) Prediction of isothermal density curves (solid lines CPA; ■ experimental data) at four different temperatures:  $T_1 = 323\text{ K}$  (blue),  $T_2 = 380\text{ K}$  (green),  $T_3 = 440\text{ K}$  (grey),  $T_4 = 480\text{ K}$  (cyan); (C) Density relative deviation as function of pressure; (D) Density relative deviation as function of temperature.

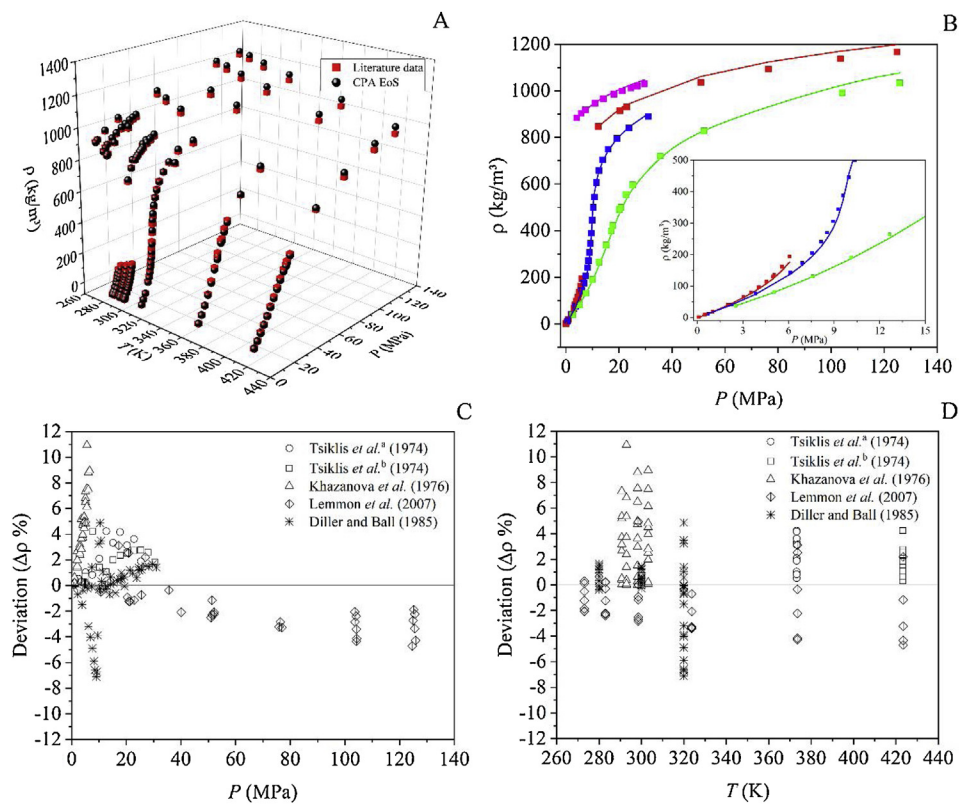


**Fig. 4.** Density of pure CO<sub>2</sub>. (A) Literature experimental data (red) and calculated from CPA EoS (black) as function of pressure and temperature; (B) Prediction of isothermal density curves (solid lines CPA; ■ experimental data) at four different temperatures: T<sub>1</sub> = 280 K (pink), T<sub>2</sub> = 298 K (red), T<sub>3</sub> = 320 K (blue), T<sub>4</sub> = 373 K (green); (C) Density relative deviation as function of pressure; (D) Density relative deviation as function of temperature.

**Table 5**

Density deviation between experimental and predicted values for pure species.

Compound	Density deviations ( $\Delta\rho$ , %)			T <sub>r</sub> range	T <sub>r</sub> range
	CPA EoS*	SRK EoS**	PR EoS**		
water	1.68	28.658	18.726	0.44 - 1.19	0.493 - 0.963
ethanol	1.59	21.141	11.004	0.39 - 0.97	0.588 - 0.973
CO <sub>2</sub>	2.44	1.206	4.348	0.89 - 1.40	0.714 - 0.986

\* This work, see Table 1.

\*\* Retrieved from Ji and Lempe [149].

calculations showed higher deviations ( $\Delta\rho = 3.53\%$  and  $\Delta\rho^{\max} = 10.94\%$ ) for these data when compared to data from others authors at similar temperature and pressure conditions. CPA EoS also showed  $\Delta\rho = 2.01\%$  and  $\Delta\rho^{\max} = 7.10\%$  considering Tsiklis et al. [86,87], Lemmon et al. [89] and Diller and Ball [90] data and discarding Khazanova et al. [88] values. If compared with cubic EoSs (SRK and PR) CPA presented an accurate description of volumetric behavior, as presented in Table 5.

For water and ethanol, densities predicted by CPA EoS were significantly better than ones predicted by original cubic EoSs, as presented in Table 5. CO<sub>2</sub> densities calculated using CPA EoS presented equivalent deviations to SRK EoS. It's noteworthy that for CPA supercritical conditions were also evaluated.

Vapor pressures and densities of water, ethanol and CO<sub>2</sub> were satisfactorily described by CPA EoS. However, critical point calculations presented significant deviations as reported in Table 6.

The deficiency observed in critical point description occurs due to the addition of association term to SRK, once cubic EoSs present accurate description of critical properties. In order to minimize critical point deviations and improve CPA predictive capacity new methodologies were proposed by Coutinho et al. [150] and Vinhal et al. [151]. Both methods include critical data restrictions in CPA

**Table 6**  
Comparison of SRK and CPA EoSs for pure compound critical point description.

	Compound	water	ethanol	CO <sub>2</sub>
Reference*	P <sub>c</sub> (MPa)	22.055	6.137	7.383
	T <sub>c</sub> (K)	647.13	513.92	304.21
	P <sub>e</sub> (MPa)	22.035	6.146	7.377
	Desv P <sub>c</sub> (%)	-0.092	0.150	-0.079
	T <sub>c</sub> (K)	647.05	513.90	304.17
	Desv T <sub>c</sub> (%)	-0.013	-0.004	-0.012
SRK EoS	P <sub>c</sub> (MPa)	31.835	9.121	9.121
	Desv P <sub>c</sub> (%)	44.346	48.623	23.540
	T <sub>c</sub> (K)	684.86	542.87	313.80
	Desv T <sub>c</sub> (%)	5.830	5.634	3.153
CPA EoS	P <sub>c</sub> (MPa)	22.055	6.137	7.383
	T <sub>c</sub> (K)	647.13	513.92	304.21
	P <sub>e</sub> (MPa)	22.035	6.146	7.377
	Desv P <sub>c</sub> (%)	-0.092	0.150	-0.079

\* Reference values were retrieved from DIPPR database [147].

parametrization procedure. However, an increase in the deviation of the saturated liquid phase volumes was reported [151].

Even though the overestimation of critical coordinates presented by original CPA, vapor pressures and densities were well predicted also near the critical region. Therefore, CPA EoS is adequate for the design of supercritical processes, e.g., reactors and supercritical fluid extraction unit, even in the vicinity of critical point.

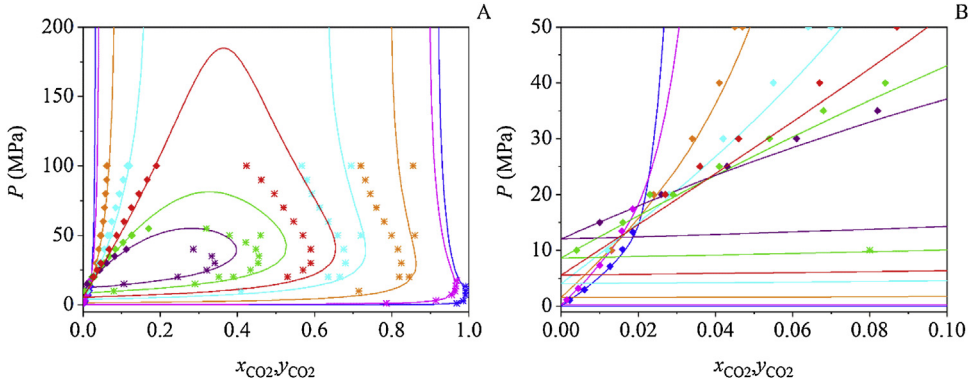


**Fig. 5.** Description of isothermal curves for the \$\text{CO}\_2\$+water system. (\$\blacklozenge\$) experimental bubble points and (\*) dew points [15,57,91–99]. Solid line: calculated curves with the CPA EoS. (A) \$P\$-\$xy\$ diagram at seven different temperatures: \$T\_1 = 348\$ K (blue, \$k\_{ij} = 0.2471\$), \$T\_2 = 398\$ K (pink, \$k\_{ij} = 0.2935\$), \$T\_3 = 473\$ K (orange, \$k\_{ij} = 0.3195\$), \$T\_4 = 523\$ K (cyan, \$k\_{ij} = 0.3089\$), \$T\_5 = 543\$ K (red, \$k\_{ij} = 0.2711\$), \$T\_6 = 573\$ K (green, \$k\_{ij} = 0.2424\$) and \$T\_7 = 598\$ K (purple, \$k\_{ij} = 0.1628\$). (B) \$P\$-\$xy\$ diagram for \$\text{CO}\_2\$ molar fraction between 0 and 0.1.

### 3.2. Binary mixtures

In order to describe the phase behavior and volumetric properties of the binary mixtures using the CPA EoS an interaction parameter was required. The interaction parameter was fitted by minimizing the following objective function using phase equilibrium data:

$$OF = \sum_{i=1}^{NDP} (y_2^{\text{exp}} E_1 - y_1^{\text{exp}} E_2)^2 + (E_1 + E_2)^2 \quad (2)$$

$$E_j = x_j^{\text{exp}} \phi_j^l - y_j^{\text{exp}} \phi_j^v \quad (3)$$

Where \$NDP\$ is the number of data points, \$j\$ denotes the component, 1 for \$\text{CO}\_2\$ and 2 for the other solvent, i.e. water or ethanol, \$\phi\_j\$ is the fugacity coefficient of component \$j\$. Superscripts \$l\$ and \$v\$ denote liquid and vapor phases, and variables \$x\$ and \$y\$ are the liquid and vapor mole fractions, respectively. It is noteworthy that some phase equilibrium is related to other fluid states of aggregation such as gas and supercritical. The application of the isofugacity criterion expressed by Eqs. (2) and (3) was found suitable for the binary interaction parameter estimation.

Interaction parameter (\$k\_{ij}\$) of \$\text{CO}\_2\$+water showed a temperature dependency and a quadratic expression was found adequate to describe phase equilibrium data in the temperature range of 278–623 K.

$$k_{\text{CO}_2,\text{water}} = -6.94365 \times 10^{-6} T^2 + 6.32 \times 10^{-3} T - 1.11335 \quad (4)$$

For \$\text{CO}\_2\$+ethanol, temperature dependency was neglected and the binary parameter obtained was \$k\_{\text{CO}\_2,\text{ethanol}} = 0.157\$.

The \$P\$-\$xy\$ diagram of the \$\text{CO}\_2\$+water system is shown in Fig. 5. The experimental data were retrieved from literature [15,57,91–99], as seen in Table 2.

The closed regions for higher temperatures denoted vapor-liquid equilibrium, while for lower temperatures a liquid-liquid region was observed (Fig. 5A). The LLE region increased along the decrease in temperature. CPA EoS was able to calculate the \$\text{CO}\_2\$-water phase behavior with accuracy, specially the regions of low \$\text{CO}\_2\$ concentration (Fig. 5B) and pressures lower than 40 MPa. For temperatures slightly lower than the critical temperature of water (647 K) a nozzle shape in the phase diagram was experimentally observed. It is noteworthy CPA EoS capability to describe this special behavior as seen in Fig. 5A (red solid line). tc-PR CEoS also represented the nozzle shape [35].

Fig. 6 presents the \$\text{CO}\_2\$+water VLE behavior obtained with CPA EoS for describing the selected experimental data collected from the literature.

The results showed satisfactory accordance with CPA. The EoS was used to calculate and compare the \$\text{CO}\_2\$+water phase behavior against nine authors for a total of 271 data points in wide ranges of pressure and temperature. The liquid and vapor mean relative deviations were \$\Delta x\_{\text{H}\_2\text{O}} = 0.49\%\$ and \$\Delta y\_{\text{CO}\_2} = 4.63\%\$. According to the results, the increase in temperature was found to be determinant in the calculated composition error. In the range 250–500 K, the observed vapor phase deviations were below 15%, with \$\Delta y\_{\text{CO}\_2} = 1.69\%\$, as showed in Fig. 6B. The liquid phase calculations were not as affected by temperature, presenting \$\Delta x\_{\text{H}\_2\text{O}} = 0.30\%\$ up to 500 K. The approach using VLE and density for CPA parametrization for the pure species and the fitted interaction parameters, Eq. (4), was not found accurate to describe \$\text{CO}\_2\$+water critical locus (\$\Delta P\_{\text{crit}} = 14.3\%\$ and \$\Delta T\_{\text{crit}} = 5.9\%\$).

The VLE data calculated by CPA presented noticeable larger deviations when compared to Takenouchi and Kennedy [99] data for the isotherms 573 and 598 K, as seen in Fig. 6A and B, with a pressure range from 10 to 60 MPa. Concerning this experimental work, CPA evidenced greater deviations along the pressure increase, as illustrated in Fig. 6A. The particular 493 K isotherm from Mueller et al. [96] presented similar behavior, however for a much lower pressure range (2.6–6.5 MPa). This indicates experimental error associated to the data set, once experimental data from other authors in similar pressure and temperature conditions were well calculated by CPA. In liquid phase composition, only two CPA calculated points, based on Todheide and Franck [15] experimental data points, presented deviation greater than 3% (Fig. 6C and D). Furthermore, for temperatures up to 500 K the CPA EoS showed significant deviations only when compared to Cai et al. [98] experimental data (Figs. 6B and 6D).

Fig. 7 presents \$\text{CO}\_2\$+water density behavior along pressure for five isotherms and the deviation between experimental and predicted data, as function of pressure and temperature.

Fig. 7 shows that the \$\text{CO}\_2\$+water density was calculated with high accuracy throughout the entire pressure and temperature ranges (\$\Delta\rho = 0.5\%\$). Tabasinejad et al. [101] presented 3 isotherms as seen in Fig. 7B, these data showed that for pressures below 40 MPa the CPA calculated densities were lower than the experimental values. For greater pressures, the opposite behavior was observed, with negative deviations. The increase in temperature also revealed higher error in the density calculation. CPA EoS demonstrated great calculation performance, with a maximum density deviation of 4.05% for Teng et al. [102] experimental data. Nighswander et al. [104] carried out measurements of density at high temperatures (353–471 K) and low pressures (2.0–10.2 MPa). Calculated densities by CPA for these data showed mean deviation of \$\Delta\rho = 1.15\%\$. Lower deviations were expected at low pressure range. However, density

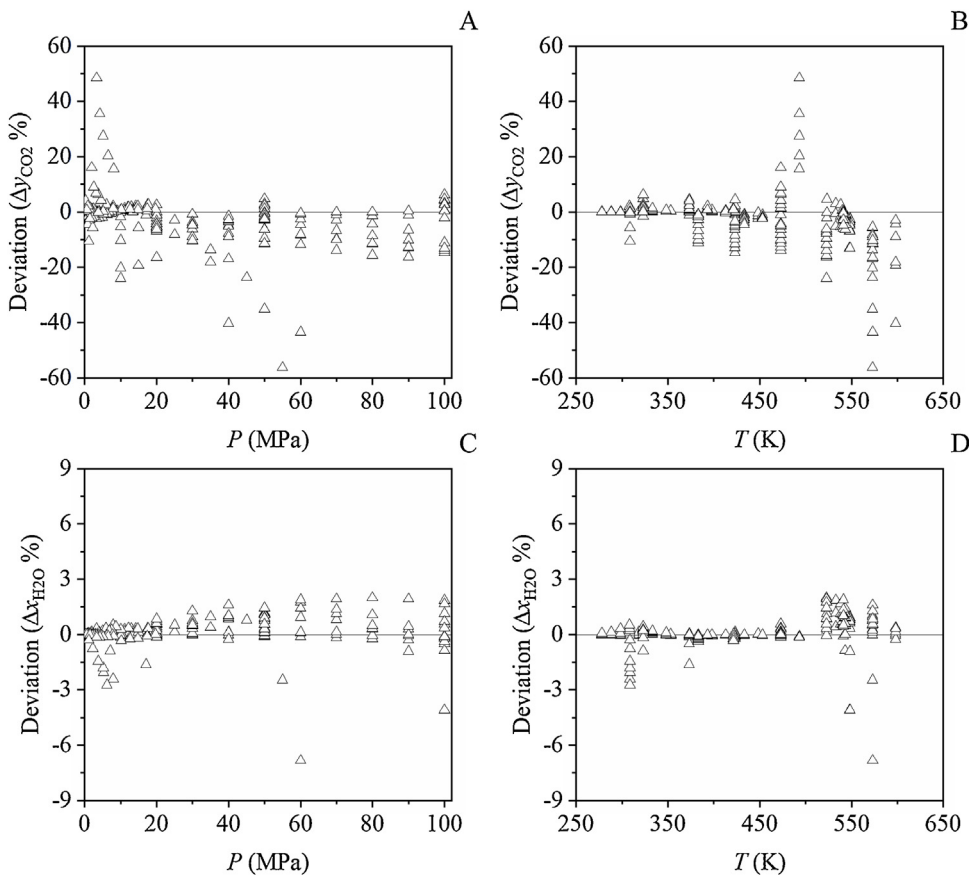


**Fig. 6.** Relative deviations for  $\text{CO}_2$ +water VLE compositions using CPA EoS ( $k_{\text{CO}_2,\text{water}}$  described by Eq. (4)). (Δ) Experimental data [15,57,91–99], see Table 2. (A) Liquid phase as function of pressure. (B) Liquid phase as function of temperature. (C) Vapor phase as function of pressure. (D) Vapor phase as function of temperature.

**Table 7**

$\text{CO}_2$ +water vapor pressure and density deviations ( $\Delta \%$ ) applying PR78 and CPA EoSs considering temperature dependence on  $k_{ij}^*$ ; experimental data reported in Table 2.

CPA	PR78		CPA	PR78	
$\Delta x_{\text{H}_2\text{O}}$	$\Delta y_{\text{CO}_2}$	$\Delta x_{\text{H}_2\text{O}}$	$\Delta y_{\text{CO}_2}$	$\Delta \rho$	$\Delta \rho$
0.49	4.63	1.31	4.08	0.5	9.82

\*  $k_{ij}$  obtained minimizing the objective function described by Eqs. (2) and (3) for each isothermal data set.

measurements were conducted at high temperatures, providing more uncertainties, see Fig. 7C. Table 7 presents vapor pressure and density deviations for  $\text{CO}_2$ +water comparing CPA and PR EoSs. CPA deviations were close to the experimental uncertainties reported in the literature [100–106].

It was observed in Table 7 that both EoSs were adequate for phase behavior description.

for  $\text{CO}_2$ +water system. Nevertheless, for volumetric behavior CPA presented a significant improvement, corroborating its applicability. For supercritical process design not only phase behavior description is determinant but volumetric behavior is also important. Thus, CPA EoS is more indicated than cubic EoS for the design and representation of supercritical processes containing  $\text{CO}_2$ +water.

The phase behavior for the  $\text{CO}_2$ +ethanol system is illustrated by the  $P$ - $x$  diagram in Fig. 8. Complete VLE experimental data were retrieved from literature [18,107–128] (see Table 2) and used to fit the binary interaction parameter.

The five isotherms presented in Fig. 8A show agreement between experimental data and CPA calculations. For the three intermediate temperatures, i.e., 313 K, 333 K and 353 K, the majority of the calculated values were lower than the experimental

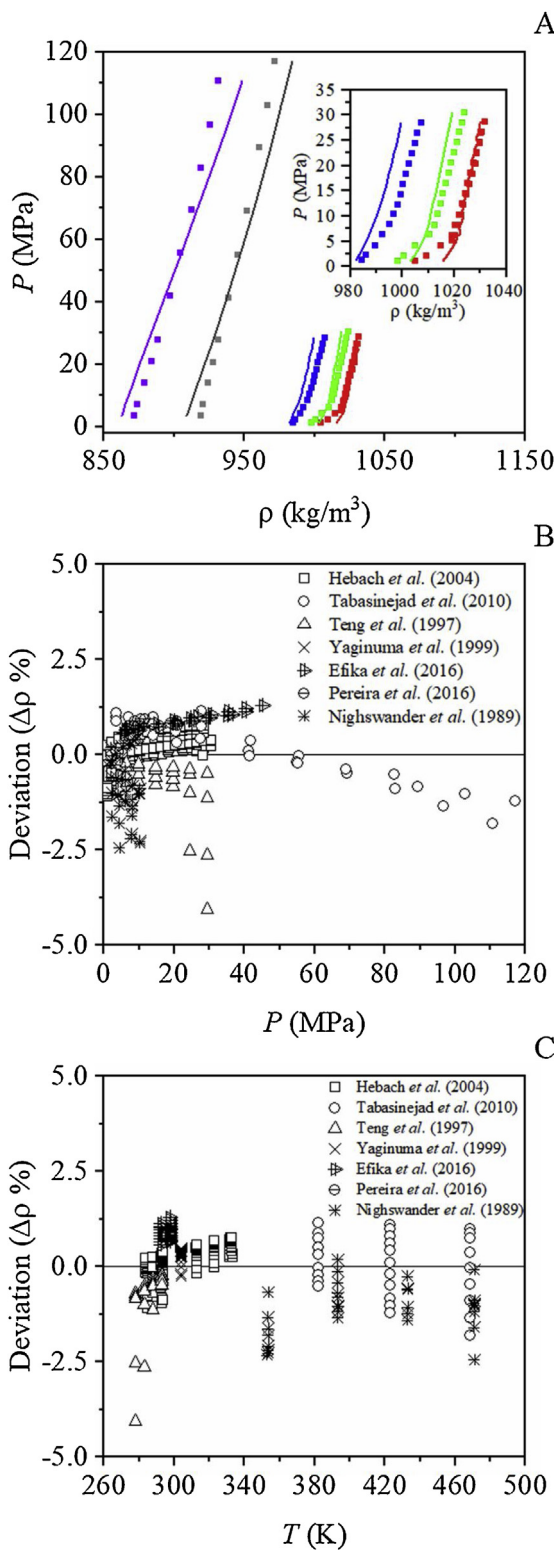
values for both dew and bubble curves. Thus, negative deviations for liquid and vapor compositions of  $\text{CO}_2$  were observed. This behavior was not noticed for 291 and 391 K isotherms. The former presented positive deviations for bubble curve and negative for dew curve. The latter presented pressure deviations from positive to negative in the bubble curve and negative along the whole dew curve, as seen in Fig. 8C.

Fig. 9 depicts phase behavior description for  $\text{CO}_2$ +ethanol system based on the deviations. It was observed accurate VLE representation by the CPA EoS only for ethanol rich mixtures ( $x_{\text{CO}_2} < 0.3$ ).

The results presented in Fig. 9 indicate that the liquid and vapor compositions for the whole data were poorly calculated ( $\Delta x_{\text{EtOH}} = 21.93\%$  and  $\Delta y_{\text{CO}_2} = 3.82\%$ ), with maximum deviations of 72.74% and 28.36% for the liquid and vapor phases, respectively. However, ethanol concentrated systems showed satisfactory results, with  $\Delta x_{\text{EtOH}} = 4.97\%$  and  $\Delta y_{\text{CO}_2} = 0.75\%$ . Fig. 9 also shows that the CPA mainly calculated mole fractions higher than the experimental values, as demonstrated by the predominant positive deviations for both phases. Negative deviations were observed only for Secuiaru et al. [18] data points. The approach using VLE and density for CPA parametrization for pure species and an adjustable binary interaction parameter was not found accurate to describe  $\text{CO}_2$ +ethanol critical locus ( $\Delta P_{\text{crit}} = 23.6\%$  and  $\Delta T_{\text{crit}} = 5.8\%$ ).

Fig. 10 illustrates the volumetric behavior results for  $\text{CO}_2$ +ethanol mixtures. CPA EoS presented satisfactory density prediction for  $\text{CO}_2$ +ethanol system, with  $\Delta \rho = 2.92\%$  and maximum deviation of 21.79%.

Density data below 6 MPa were better described ( $\Delta \rho = 1.68\%$  and  $\Delta \rho^{\text{max}} = 5.86\%$ ) when compared to the total pressure range, as seen in Fig. 10A and 10B. It is interesting to highlight that this



**Fig. 7.**  $\text{CO}_2$ +water density. (A) Prediction of five isothermal curves (solid line;  $k_{\text{CO}_2,\text{water}}$  described by Eq. (4)) and experimental data points (■) at  $T_1 = 284 \text{ K}$  (red),  $T_2 = 302 \text{ K}$  (green),  $T_3 = 332 \text{ K}$  (blue),  $T_4 = 423 \text{ K}$  (grey),  $T_5 = 468 \text{ K}$  (violet). (B) Density relative deviations as function of pressure. (C) Density relative deviation as function of temperature.

behavior was noticed close to ethanol's critical pressure (6.4 MPa). For greater pressures, CPA calculated densities with deviations between 5% and 21.8% for Seifried and Temelli [132], Chiehming et al. [44] and Tsivintzelis et al. [133] experimental data.

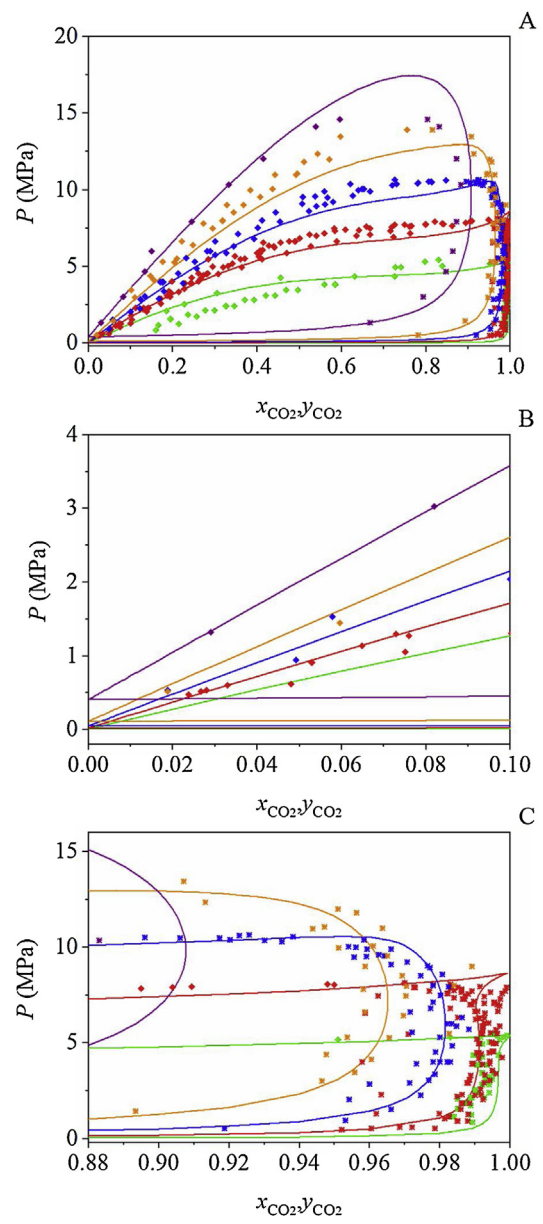


**Fig. 8.** Prediction of isothermal curves for the  $\text{CO}_2$ +ethanol system ( $k_{\text{CO}_2,\text{ethanol}} = 0.157$ ). (♦) experimental bubble points, (\*) experimental dew points. Solid line: predicted curves with the CPA EoS. (A)  $P$ - $x$  diagram at five different temperatures:  $T_1 = 291 \text{ K}$  (green),  $T_2 = 313 \text{ K}$  (red),  $T_3 = 333 \text{ K}$  (blue),  $T_4 = 353 \text{ K}$  (orange),  $T_5 = 391 \text{ K}$  (purple). (B)  $P$ - $x$  diagram for  $\text{CO}_2$  molar fraction between 0 and 0.1. (C)  $P$ - $x$  diagram for  $\text{CO}_2$  molar fraction between 0.88 and 1.

A relation between the CPA deviation and temperature was not found for  $\text{CO}_2$ +ethanol density, regarding that narrow range (60 K). The entire temperature range showed resembling density deviations, as presented in Fig. 10 C. The EoS calculations presented high deviations in comparison to Seifried and Temelli [132] data at the particular 328 K isotherm. This may be related to experimental errors, once these authors obtained better results at higher pressures (c.a. 11 MPa) and temperature (343 K). Table 8 presents vapor pressure and density deviations for  $\text{CO}_2$ +water comparing CPA and original PR78. CPA deviations were close to the experimental density uncertainties reported in the literature. For vapor and liquid phase compositions, deviations observed were also slightly above the uncertainties reported.

PR78 presented slightly better results for phase behavior description of the  $\text{CO}_2$ +ethanol system. But CPA EoS also described

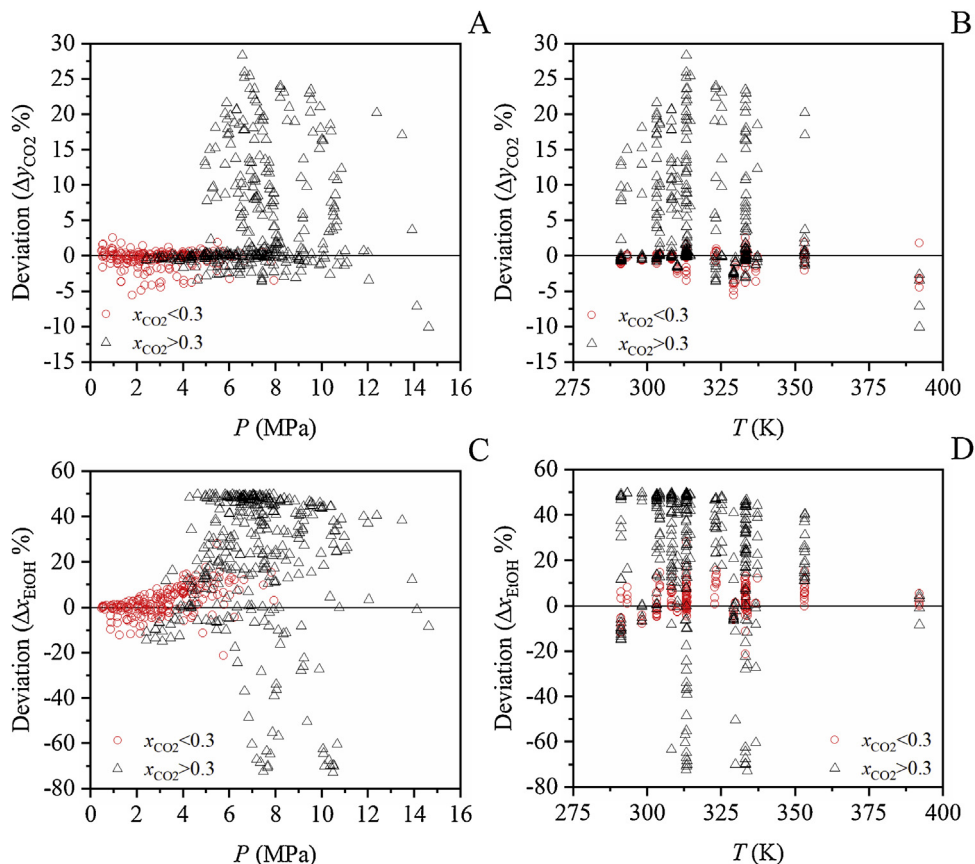


**Fig. 9.** Relative deviations for VLE compositions using CPA EoS ( $k_{\text{CO}_2, \text{ethanol}} = 0.157$ ) for the  $\text{CO}_2$ +ethanol system. Experimental data [18,107–128], see Table 2. (A) Liquid phase as function of pressure. (B) Liquid phase as function of temperature. (C) Vapor phase as function of pressure. (D) Vapor phase as function of temperature (D).

**Table 8**

$\text{CO}_2$ +ethanol vapor pressure and density deviations ( $\Delta$  %) applying PR78 and CPA EoSs neglecting temperature dependence on  $k_{ij}$ \*; experimental data reported in Table 2.

CPA	PR78	CPA	PR78
$\Delta x_{\text{EtOH}}$ 21.93	$\Delta y_{\text{CO}_2}$ 3.82	$\Delta x_{\text{EtOH}}$ 18.26	$\Delta y_{\text{CO}_2}$ 0.73

\*  $k_{ij}$  obtained minimizing the objective function described by Eqs. (2) and (3).

satisfactorily phase behavior. For density, CPA mean deviations were lower than the ones obtained for PR78 EoS. Furthermore, maximum density deviations presented a significant decrease, from 29.88% (PR78) to 21.79% (CPA). For  $\text{CO}_2$ +ethanol, original CPA could be used for describing mixture phase behavior for  $\text{CO}_2$  molar concentrations up to 0.3. For volumetric behavior representation CPA EoS is more adequate than cubic EoSs and could be applied for the complete composition range.

#### 4. Conclusion

A literature database of phase behavior and volumetric properties for  $\text{CO}_2$ +water,  $\text{CO}_2$ +ethanol and pure compounds was built. The CPA EoS applicability was demonstrated for the description of phase behavior and volumetric properties of  $\text{CO}_2$ +water and  $\text{CO}_2$ +ethanol and pure compounds over an extensive range of temperature and pressure. 4C association scheme was used for water and carbon dioxide while 2B for ethanol. Pure component parameters were retrieved from literature and binary interaction parameters were fitted to experimental phase equilibrium data. For  $\text{CO}_2$ +water, a quadratic temperature dependency on the interac-

tion parameter was found necessary. For  $\text{CO}_2$ +ethanol temperature dependency was neglected, the adjusted interaction parameter was 0.157. The results obtained with CPA EoS for pure components were compared with SRK and PR EoSs retrieved from literature. For binary mixtures, CPA was compared with PR78.

For pure components, bubble temperature was satisfactorily described presenting average deviations up to 0.25%. Agreement between references was observed for the reported experimental data. As expected, for density it was observed higher deviations, due to higher experimental uncertainties and scattering.

In relation to the binary systems,  $\text{CO}_2$ +water VLE data were adequately described by CPA EoS. The liquid phase composition was calculated with errors less than 7%. The vapor composition presented deviations mostly in the range of 15%. The density of  $\text{CO}_2$ +water system was calculated with deviations less than 5% for the entire pressure and temperature range evaluated.  $\text{CO}_2$ +ethanol VLE calculated values presented acceptable deviations only for rich ethanol concentrations ( $x_{\text{CO}_2} < 0.3$ ), with composition deviations up to 15% for both phases. For the  $\text{CO}_2$ +ethanol, density calculations resulted in small deviations, less than 5%, up to ethanol's critical pressure (6.4 MPa). For higher pressures, deviations increased up to 21%.

Despite the low accuracy of pure component critical point and binary mixtures critical locus description, CPA demonstrated a satisfactory performance for phase behavior and density calculations near this region. It was also demonstrated that CPA presented better performance than the other cubic EoSs, as expected. Thus, results indicated the applicability of the CPA EoS for phase behavior and saturated liquid density description of the pure components and the binary systems in wide temperature and pressure ranges.

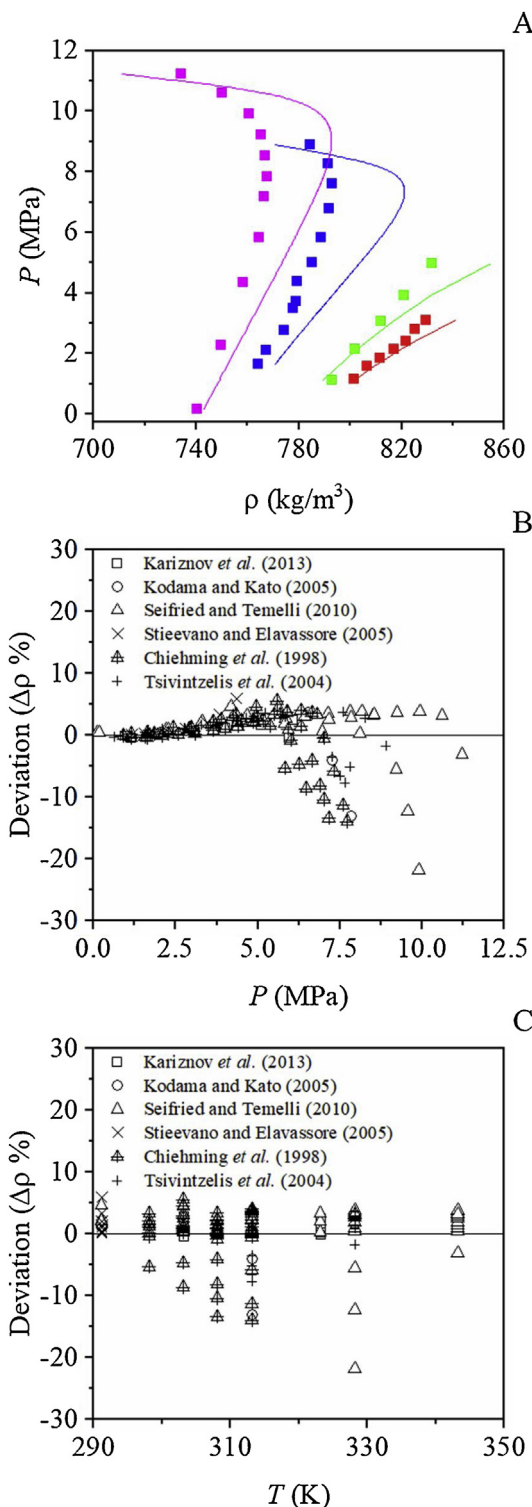


**Fig. 10.**  $\text{CO}_2$ +ethanol density. (A) Prediction of four isothermal curves (solid line;  $k_{\text{CO}_2,\text{ethanol}} = 0.157$ ) and experimental data points (■) at  $T_1 = 291 \text{ K}$  (red),  $T_2 = 303 \text{ K}$  (green),  $T_3 = 328 \text{ K}$  (blue),  $T_4 = 343 \text{ K}$  (pink). (B) Density relative deviations as function of pressure. (C) Density relative deviation function of temperature.

#### Declaration of Competing Interest

The authors declare that they have no known competing financial interests or personal relationships that could have appeared to influence the work reported in this paper.

#### Acknowledgements

The authors are grateful to Leopoldo Américo Miguez de Mello Research and Development Center (CENPES-Petrobras), Brazilian National Council for Scientific and Technological Development (CNPq), Coordination for the Improvement of Higher Education Personnel (CAPES), and National Agency for Petroleum, Natural Gas, and Biofuels (ANP) for the financial support.

#### References

- [1] F.A.V. Ferreira, T.C.S. Barbalho, H.N.M. Oliveira, O. Chiavone-Filho, Vapor-Liquid equilibrium measurements for carbon dioxide + cyclohexene + squalane at high pressures using a synthetic method, *J. Chem. Eng. Data* 62 (2017) 1456–1463, <http://dx.doi.org/10.1021/acs.jced.6b01018>.
- [2] COPPE, Revista COPPE "Corrida Para O mar," *Revista Coppe*, 2009, pp. 52.
- [3] A. Danesh, D.-H. Xu, A.C. Todd, Comparative study of cubic equations of state for predicting phase behaviour and volumetric properties of injection gas-reservoir oil systems, *Fluid Phase Equilib.* 63 (1991) 259–278, [http://dx.doi.org/10.1016/0378-3812\(91\)80036-U](http://dx.doi.org/10.1016/0378-3812(91)80036-U).
- [4] M.B. Oliveira, A.J. Queimada, G.M. Kontogeorgis, J.A.P. Coutinho, Evaluation of the  $\text{CO}_2$  behavior in binary mixtures with alkanes, alcohols, acids and esters using the Cubic-Plus-Association Equation of State, *J. Supercrit. Fluids* 55 (2011) 876–892, <http://dx.doi.org/10.1016/j.supflu.2010.09.036>.
- [5] Z. Shouqin, Z. Junjie, W. Changzhen, Novel high pressure extraction technology, *Int. J. Pharm.* 278 (2004) 471–474, <http://dx.doi.org/10.1016/j.ijpharm.2004.02.029>.
- [6] L.T. Taylor, *Supercritical Fluid Extraction*, John Wiley & Sons Inc., Canada, 1996, pp. 180.
- [7] M.P. Ekart, K.L. Bennett, S.M. Ekart, G.S. Gurdial, C.L. Liotta, C.A. Eckert, Cosolvent interactions in supercritical fluid solutions, *AIChE J.* 39 (1993) 235–248, <http://dx.doi.org/10.1002/aic.690390206>.
- [8] V. Vandana, A.S. Teja, L.H. Zalkov, Supercritical extraction and HPLC analysis of taxol from *Taxus brevifolia* using nitrous oxide and nitrous oxide+Ethanol mixtures, *Fluid Phase Equilib.* 116 (1996) 162–169, [http://dx.doi.org/10.1016/0378-3812\(96\)02991-3](http://dx.doi.org/10.1016/0378-3812(96)02991-3).
- [9] M.E.P. McNally, J.R. Wheeler, Supercritical fluid extraction coupled with supercritical fluid chromatography for the separation of sulfonylurea herbicides and their metabolites from complex matrices, *J. Chromatogr. A* 435 (1988) 63–71, [http://dx.doi.org/10.1016/S0021-9673\(01\)82163-4](http://dx.doi.org/10.1016/S0021-9673(01)82163-4).
- [10] V. Lopez-Avila, J. Benedicto, Supercritical Fluid extraction of Kava lactones from Piper methysticum (kava) herb, *J. Sep. Sci.* 20 (1997) 555–559, <http://dx.doi.org/10.1002/jhrc.1240201007>.
- [11] C. Moon-Kyoon, S. Hye-Won, L. Huen, L. Jang-Ryol, Supercritical fluid extraction of taxol and baccatin III from needles of *Taxus cuspidata*, *Biotechnol. Tech.* 8 (1994) 547–550, <http://dx.doi.org/10.1007/BF00152143>.
- [12] O. Lang, C.M. Wai, Supercritical fluid extraction in herbal and natural product studies: a practical review, *Talanta* 53 (2001) 771–782, [http://dx.doi.org/10.1016/S0039-9140\(00\)00557-9](http://dx.doi.org/10.1016/S0039-9140(00)00557-9).
- [13] R.L. Scott, P.H. van Konynenburg, Static properties of solutions. Van der Waals and related models for hydrocarbon mixtures, *Discuss. Faraday Soc.* 49 (1970) 87–97.
- [14] Saif Z.S. Al Ghafri, Esther Forte, Geoffrey C. Maitland, José Rodriguez-Henriquez, J.P. Martin Trusler, Experimental and modeling study of the phase behavior of (Methane +  $\text{CO}_2$  + water) mixtures, *J. Phys. Chem. B* 118 (2014) 14461–14478, <http://dx.doi.org/10.1021/jp509678g>.
- [15] K. Todheide, E.U.Z. Franck, Two-phase range and the critical curve in the system carbon dioxide-water up to 3500 bar, *Phys. Chem.* 37 (1963) 387–401.
- [16] V. Feriou, S. Sima, D. Geană, High pressure phase equilibrium in carbon dioxide+Ethanol system, *U.P.B. Sci. Bull., Series B* 75 (2013) 53–62.
- [17] J. Zhang, X. Wu, W. Cao, Phase equilibrium properties of supercritical carbon dioxide in binary system, *Gaodeng Xuejiao Huaxue Xuebao*. 23 (2002) 10.
- [18] V. Secuiaru, D. Feriou, Geancența, Phase behavior for carbon dioxide + ethanol system: Experimental measurements and modeling with a cubic equation of state, *J. Supercrit. Fluids* 47 (2008) 109–116, <http://dx.doi.org/10.1016/j.supflu.2008.08.004>.
- [19] P.H. van Konynenburg, R.L. Scott, J.S. Rowlinson, Critical lines and phase equilibria in binary van der Waals mixtures, *Philos. Trans. Royal Soc. A, Mathematical and Physical Sciences*. 298 (1980) 495–540, <http://dx.doi.org/10.1098/rsta.1980.0266>.
- [20] R. Privat, J.N. Jaubert, Classification of global fluid-phase equilibrium behaviors in binary systems, *Chem. Eng. Res. Des.* 91 (2013) 1807–1839, <http://dx.doi.org/10.1016/j.cherd.2013.06.026>.
- [21] S. Rowlinson, F.L. Swinton, *Liquids and Liquid Mixtures*, third ed., Butterworths Monographs in Chemistry, London, 1992.
- [22] G.M. Kontogeorgis, E.C. Voutsas, I.V. Yakoumis, D.P. Tassios, An equation of state for associating fluids, *Ind. Eng. Chem. Res.* 35 (1996) 4310–4318, <http://dx.doi.org/10.1021/ie9600203>.
- [23] I.V. Yakoumis, G.M. Kontogeorgis, E.C. Voutsas, D.P. Tassios, Vapor-liquid equilibria for alcohol/hydrocarbon systems using the CPA equation of state,

- Fluid Phase Equilib. 130 (1997) 31–47, [http://dx.doi.org/10.1016/S0378-3812\(96\)03200-1](http://dx.doi.org/10.1016/S0378-3812(96)03200-1).
- [24] S.H. Huang, M. Radosz, Equation of state for small, large, polydisperse, and associating molecules: extension to fluid mixtures, Ind. Eng. Chem. Res. 30 (1991) 1994–2005, <http://dx.doi.org/10.1021/ie00056a050>.
- [25] I.V. Yakoumis, G.M. Kontogeorgis, E.C. Voutsas, E.M. Hendriks, D.P. Tassios, Prediction of phase equilibria in binary aqueous systems containing alkanes, cycloalkanes, and alkenes with the cubic-plus-association equation of state, Ind. Eng. Chem. Res. 37 (1998) 4175–4182, <http://dx.doi.org/10.1021/ie970947i>.
- [26] C. Perakis, E. Voutsas, K. Magoulas, D. Tassios, Thermodynamic modelling of the vapor-liquid equilibrium of the water/ethanol/CO<sub>2</sub> system, Fluid Phase Equilib. 243 (2006) 142–150, <http://dx.doi.org/10.1016/j.fluid.2006.02.018>.
- [27] C. Perakis, E. Voutsas, K. Magoulas, D. Tassios, Thermodynamic modelling of the water + acetic acid + CO<sub>2</sub> system: the importance of the number of association sites of water and of the nonassociation contribution for the CPA and SAFT-type models, Ind. Eng. Chem. Res. 46 (2007) 932–938, <http://dx.doi.org/10.1021/ie0609416>.
- [28] I. Tsivintzelis, G.M. Kontogeorgis, M.L. Michelsen, E.H. Stenby, Modeling phase equilibria for acid gas mixtures using the CPA equation of state. Part II: Binary mixtures with CO<sub>2</sub>, Fluid Phase Equilib. 306 (2011) 38–56, <http://dx.doi.org/10.1016/j.fluid.2011.02.006>.
- [29] J.O. Valderrama, The State of the Cubic Equations of State, Ind. Eng. Chem. Res. 42 (2003) 1603–1618, <http://dx.doi.org/10.1021/ie020447b>.
- [30] A. Fenghour, W.A. Wakeham, J.T.R. Watson, Densities of (water + carbon dioxide) in the temperature range 415 K to 700 K and pressures up to 35 MPa, J. Chem. Thermodyn. 28 (1996) 433–446, <http://dx.doi.org/10.1006/jcht.1996.0043>.
- [31] S. Hou, G.C. Maitland, J.P.M. Trusler, Measurement and modeling of the phase behavior of the (carbon dioxide + water) mixture at temperatures from 298.15 K to 448.15 K, J. Supercrit. Fluids 73 (2013) 87–96, <http://dx.doi.org/10.1016/j.supflu.2012.11.011>.
- [32] J.W. Qian, J.N. Jaubert, R. Privat, Phase equilibria in hydrogen-containing binary systems modeled with the Peng–Robinson equation of state and temperature-dependent binary interaction parameters calculated through a group-contribution method, J. Supercrit. Fluids 75 (2013) 58–71, <http://dx.doi.org/10.1016/j.supflu.2012.12.014>.
- [33] S. Vitu, R. Privat, J.N. Jaubert, F. Mutelet, Predicting the phase equilibria of CO<sub>2</sub>+hydrocarbon systems with the PPR78 model (PR EOS and kij calculated through a group contribution method), J. Supercrit. Fluids 45 (2008) 1–26, <http://dx.doi.org/10.1016/j.supflu.2007.11.015>.
- [34] N. Jaubert, F. Mutelet, VLE predictions with the Peng–Robinson equation of state and temperature dependent kij calculated through a group contribution method, Fluid Phase Equilib. 224 (2004) 285–304, <http://dx.doi.org/10.1016/j.fluid.2004.06.059>.
- [35] J.W. Qian, R. Privat, J.N. Jaubert, Predicting the phase equilibria, critical phenomena, and mixing enthalpies of binary aqueous systems containing alkanes, Cycloalkanes, aromatics, Alkenes, and gases (N<sub>2</sub>, CO<sub>2</sub>, H<sub>2</sub>S, H<sub>2</sub>) with the PPR78 equation of state, Ind. Eng. Chem. Res. 52 (2013) 16457–16490, <http://dx.doi.org/10.1021/ie402541h>.
- [36] G.D. Pappa, C. Perakis, I.N. Tsimpanogiannis, E.C. Voutsas, Thermodynamic modeling of the vapor-liquid equilibrium of the CO<sub>2</sub>/H<sub>2</sub>O mixture, Fluid Phase Equilib. 284 (2009) 56–63, <http://dx.doi.org/10.1016/j.fluid.2009.06.011>.
- [37] S. Aparicio-Martínez, K.R. Hall, Phase equilibria in water containing binary systems from molecular based equations of state, Fluid Phase Equilib. 254 (2007) 112–125, <http://dx.doi.org/10.1016/j.fluid.2007.02.030>.
- [38] A. Aasen, M. Hammer, G. Skaugen, J.P. Jakobsen, Wilhelmsen, Thermodynamic models to accurately describe the PVTxy-behavior of water/carbon dioxide mixtures, Fluid Phase Equilib. 442 (2017) 125–139, <http://dx.doi.org/10.1016/j.fluid.2017.02.006>.
- [39] E. Perfetti, R. Thiery, J. Dubessy, Equation of state taking into account dipolar interactions and association by hydrogen bonding: II-Modelling liquid-vapour equilibria in the H<sub>2</sub>O-H<sub>2</sub>S, H<sub>2</sub>O-CH<sub>4</sub> AND H<sub>2</sub>O-CO<sub>2</sub> systems, Chem. Geol. 251 (2008) 50–57, <http://dx.doi.org/10.1016/j.chemgeo.2008.02.012>.
- [40] A.J. Hadi, Gas-liquid equilibrium prediction of CO<sub>2</sub>-Ethanol system at moderate pressures and different temperatures, Diyala Journal of Engineering Sciences. 3 (2010) 91–106, ISSN 1999-8716.
- [41] M. Kariznovi, H. Nourozieh, J. Abedi, Experimental measurements and predictions of density, viscosity, and carbon dioxide solubility in methanol, ethanol, and 1-propanol, J. Chem. Thermodyn. 57 (2013) 408–415, <http://dx.doi.org/10.1016/j.jct.2012.10.002>.
- [42] M. Stievano, N. Elvassore, High-pressure density and vapor–liquid equilibrium for the binary systems carbon dioxide–ethanol, carbon dioxide–acetone and carbon dioxide–dichloromethane, J. Supercrit. Fluids 33 (2005) 7–14, <http://dx.doi.org/10.1016/j.supflu.2004.04.003>.
- [43] S.H. Huang, M. Radosz, Equation of state for small, large, polydisperse and associating molecules, Ind. Eng. Chem. Res. 29 (1990) 2284–2294, <http://dx.doi.org/10.1021/ie00107a014>.
- [44] J.C. Chiehming, C. Kou-Lung, D. Chang-Yih, A new apparatus for the determination of P–x–y diagrams and Henry's constants in high pressure alcohols with critical carbon dioxide, J. Supercrit. Fluids 12 (1998) 223–237, [http://dx.doi.org/10.1016/S0896-8446\(98\)00076-X](http://dx.doi.org/10.1016/S0896-8446(98)00076-X).
- [45] S. Hirohama, T. Takatsuka, S. Miyamoto, T. Muto, Measurement and Correlation of Phase Equilibria for the Carbon Dioxide-Ethanol-Water system, J. Chem. Eng. Jpn. 26 (1993) 408–415, <http://dx.doi.org/10.1252/jce.26.408>.
- [46] M.B. Oliveira, A.J. Queimada, J.A.P. Coutinho, Prediction of near and supercritical fatty acid ester+alcohol systems with the CPA EoS, J. Supercrit. Fluids 52 (2010) 241–248, <http://dx.doi.org/10.1016/j.supflu.2010.01.014>.
- [47] V.N. Chukanov, V.P. Skripov, Spezifische Volumina vom überhitzten Wasser, Teplofiz.Vys.Temp. 9 (1971) 739–745.
- [48] V.N. Evstefeev, V.N. Chukanov, V.P. Skripov, Spezifische Volumina vom überhitzten Wasser, Teplofiz.Vys.Temp. 15 (1977) 659–661.
- [49] A.N. Gubkov, N.A. Fermor, N.I. Smirnov, Vapor pressure of mono-poly systems, Zhurnal Prikl. Khim. 37 (1964) 2204–2210.
- [50] S.L. Rivkin, G.V. Troyanovskaya, T.S. Akhundov, Experimentelle untersuchung der spezifischen Volumina Von Wasser, Teplofiz.Vys.Temp. 2 (1964) 219–229.
- [51] D. Ambrose, I.J. Lawrenson, The vapour pressure of water, The J. of Chem. Thermodynamics. 4 (1972) 755–761, [http://dx.doi.org/10.1016/0021-9614\(72\)90049-3](http://dx.doi.org/10.1016/0021-9614(72)90049-3).
- [52] M.O. Maggioli, F.J. Passamonti, A.C. Chialvo, Vapor pressure of saturated aqueous solutions of potassium sulfate from 310 K to 345 K, J. Thermodyn. 4 (2011) (2011), <http://dx.doi.org/10.1155/2011/432132>.
- [53] A. Ure, W.H. Wollaston, New experimental researches on some of the leading doctrines of calorific; particularly on the relation between the elasticity, temperature, and latent heat of different vapours; and on thermometric admeasurement and capacity, Philos. Trans. Biol. Sci. 108 (1818), <http://dx.doi.org/10.1089/rstl.1818.0020>, vi–vi.
- [54] N.S. Osborne, H.F. Stimson, E.F. Flock, D.C.J. Ginnings, The Pressure of Saturated Water Vapor in the Range 100 deg to 374 deg, Res. Natl. Bur. Stand. 10 (1933) 155.
- [55] A.M. Sirota, Constant pressure heat capacity of water at saturation curve, Inzh.-Fiz. Zh. 6 (1963) 52–55.
- [56] M. Abdulagatov, Azizov Ilmutdin, D. Nazim, Experimental vapor pressures and derived thermodynamic properties of aqueous solutions of Lithium nitrate from 423 to 623 K, J. Solution Chem. 33 (2004) 1517–1537, <http://dx.doi.org/10.1007/s10953-004-1405-9>.
- [57] D.R. Douslin, Vapor pressure of water from –2.5 to 20°C, J. Chem. Thermodyn. 3 (1971) 187–193, [http://dx.doi.org/10.1016/S0021-9614\(71\)80101-5](http://dx.doi.org/10.1016/S0021-9614(71)80101-5).
- [58] V.A. Borzunov, V.N. Razumikhin, V.A. Stekolnikov, Bestimmung der Dichte von n-Hexan und Wasser bei Drücken bis 10000 kg/cm<sup>2</sup>, Teplofiz.Svoistva Vesh.Mater. (1970) 146–152.
- [59] S.L. Rivkin, T.S. Akhundov, Experimentelle untersuchung der spezifischen Volumina Von Wasser, Teploenergetika (1962) 57–65.
- [60] H. Kubota, S. Tsuda, M. Murata, T. Yamamoto, Y. Tanaka, T. Makita, Specific volume and viscosity of methanol-water mixtures under high pressure, The Review of Physical Chemistry of Japan 49 (1980) <http://hdl.handle.net/2433/47079>.
- [61] B. Guignon, C. Aparicio, P.D. Sanz, Specific volume of liquid water from (253 to 323) K and pressures up to 350 MPa by volumetric measurements, J. Chem. Eng. Data 55 (2010) 3338–3345, <http://dx.doi.org/10.1021/je100083w>.
- [62] K. Tanishita, J. Watanabe, H. Kijima, K. Ishii, M. Oguchi, Uematsu, Experimental study of the p, V, T properties of water for temperatures in the range 323.15 to 773.15 K and pressures up to 200 MPa, J. Chem. Thermodyn. 8 (1976) 1–20, [http://dx.doi.org/10.1016/0021-9614\(76\)90144-0](http://dx.doi.org/10.1016/0021-9614(76)90144-0).
- [63] G.S. Kelly, G.E. McLaurin, E. Whalley, W.G. Schneider, PVT properties of water – VII. Vapour densities of light and heavy water from 150 to 500°C, Proc. R. Soc. Lond. A. 425 (1989) 1–16, <http://dx.doi.org/10.1098/rspa.1989.0098>.
- [64] K.P. Mishchenko, V.V. Subbotina, Zh.Prikl.Khim. 40 (1967) 1156–1159.
- [65] W.A. Kahlbaum, C.G. von Wirkner, Monograph, Basel (1897) 1–222.
- [66] G. Scatchard, G. Satkiewicz, Frank, Vapor–Liquid Equilibrium. XII. The System Ethanol-Cyclohexane from 5 to 65°, J. Am. Chem. Soc. 86 (1964) 130–133, <http://dx.doi.org/10.1021/ja01056a003>.
- [67] D.D. Kalafati, D.S. Rasskazov, E.K. Petrov, The Pressure, Volume, Temperature Functions of Ethyl Alcohol, Teploenergetika 14 (1967) 77–81.
- [68] P.G. McCracken, T.S. Storwick, J.M.J. Smith, Phase Behavior from Enthalpy Measurements. Benzene-Ethyl Alcohol and n-Pentane-Ethyl Alcohol Systems, Ind. Eng. Chem. Eng. Data Ser. 5 (1960) 130–132, <http://dx.doi.org/10.1021/je60006a002>.
- [69] S. Young, The Internal Heat of Vaporization constants of thirty pure substances, Sci. Proc. R. Dublin Soc. 12 (1910) 374–443.
- [70] D. Ambrose, C.H.S. Sprake, R. Townsend, Thermodynamic properties of organic oxygen compounds XXXVII. Vapour pressures of methanol, ethanol, pentan-1-ol, and octan-1-ol from the normal boiling temperature to the critical temperature, J. Chem. Thermodyn. 7 (1975) 185–190, [http://dx.doi.org/10.1016/0021-9614\(75\)90267-0](http://dx.doi.org/10.1016/0021-9614(75)90267-0).
- [71] P. Reddy, J. David Raal, D. Ramjugernath, A novel dynamic recirculating apparatus for vapour–liquid equilibrium measurements at moderate pressures and temperatures, Fluid Phase Equilib. 358 (2013) 121–130, <http://dx.doi.org/10.1016/j.fluid.2013.07.044>.
- [72] P. Susial, A. Sosa-Rosario, J.J. Rodriguez-Henriquez, R.J. Rios-Santana, Vapor pressure and VLE data measurements on ethyl Acetate/Ethanol binary system at 0.1, 0.5, and 0.7 MPa, Chem. Eng. Jpn. 44 (2011) 155–163, <http://dx.doi.org/10.1252/jcej.10we176>.
- [73] G. Scatchard, C.L. Raymond, Vapor–Liquid Equilibrium. II. Chloroform–Ethanol Mixtures at 35, 45 and 55°, J. Am. Chem. Soc. 60 (1938) 1278–1287, <http://dx.doi.org/10.1021/ja01273a002>.

- [74] C.B. Kretschmer, R. Wiebe, Liquid-vapor equilibrium of ethanol-toluene solutions, *J. Am. Chem. Soc.* 71 (1949) 1793–1797, <http://dx.doi.org/10.1021/ja01173a076>.
- [75] Peter Sauermann, Klaus Holzapfel, Jörn Oprzynski, Friedrich Kohler, Wim Poot, Theodoor W. de Loos, The  $p\varrho T$  properties of ethanol + hexane, *Fluid Phase Equilib.* 112 (1995) 249–272, [http://dx.doi.org/10.1016/0378-3812\(95\)02798-J](http://dx.doi.org/10.1016/0378-3812(95)02798-J).
- [76] I.F. Golubev, T.N. Vasilkovskaya, V.S. Zolin, *Inzh.Fiz.Zh.* 38 (1980) 668–670.
- [77] Y. Takiguchi, M. Uematsu, Densities for liquid ethanol in the temperature range from 310 K to 480 K at pressures up to 200 MPa, *J. Chem. Thermodyn.* 28 (1996) 7–16, <http://dx.doi.org/10.1006/jcht.1996.0003>.
- [78] H. Kubota, Y. Tanaka, T. Makita, Volumetric behavior of pure alcohols and their water mixtures under high pressure, *Int. J. Thermophys.* 8 (1987) 47–70, <http://dx.doi.org/10.1007/BF00503224>.
- [79] Y. Tanaka, T. Yamamoto, Y. Satomi, H. Kubota, T. Makita, Specific volume and viscosity of ethanol-water mixtures under high pressure, *Rev. Phys. Chem. Jpn.* 47 (1977) 12–24 <http://hdl.handle.net/2433/47042>.
- [80] B. Yuçelen, A.J. Kidney, Vapor-Liquid Equilibria in the Nitrogen + Carbon Dioxide + Propane System from 240 to 330 K at Pressures to 15 MPa, *J. Chem. Eng. Data* 44 (1999) 926–931, <http://dx.doi.org/10.1021/je980321e>.
- [81] V.G. Matviienko, N.L. Yarym-Agaev, Vapor-liquid equilibrium and volumetric properties of the liquid phase of the gamma-butyrolactone-carbon dioxide system at increasing pressures, *Zhurnal Prikl. Khim.* 72 (1999) 1085–1089.
- [82] J.R. Roebrick, T.A. Murrell, E.E. Miller, The joule-thomson effect in carbon dioxide, *J. Am. Chem. Soc.* 64 (1942) 400–411, <http://dx.doi.org/10.1021/ja01254a048>.
- [83] J.G. Harris, K.H. Yung, Carbon dioxide's liquid-vapor coexistence curve and critical properties as predicted by a simple molecular model, *J. Phys. Chem.* 99 (1995) 12021–12024, <http://dx.doi.org/10.1021/j100031a034>.
- [84] G. Di Nicola, G. Giuliani, F. Polonara, R. Stryjek, Solid-liquid equilibria for the CO<sub>2</sub> + R125 and N<sub>2</sub>O + R125 systems: a new apparatus, *J. Chem. Eng. Data* 51 (2006) 2209–2214.
- [85] J.F. Ely, J.W. Magee, W.M. Haynes, GPA Research Rep., Rep.No. RR-110, 1987, pp. 1–161.
- [86] D.S. Tsiklis, L.R. Linshits, I.B. Rodkina, Untersuchung der Volumeigenschaften von Gas-Mischungen. I. Molvolumina und zweite Virialkoeffiziente der CO<sub>2</sub>-He-Mischungen bei 100° C, *Zh.Fiz.Khim.* 48 (1974) 1541–1544.
- [87] D.S. Tsiklis, L.R. Linshits, I.B. Rodkina, Untersuchung der Volumeigenschaften von Gas-Mischungen. I. Molvolumina und zweite Virialkoeffiziente der CO<sub>2</sub>-He-Mischungen bei 150° C, *Zh.Fiz.Khim.* 48 (1974) 1544–1546.
- [88] N.E. Khazanova, E.E. Sominskaya, A.V. Zakharova, M.B. Rozovski, *Teplofiz.Svoistva Vesh.Mater.* 10 (1976) 213–219.
- [89] E.W. Lemmon, NIST Standard Reference Database 23: Reference Fluid Thermodynamic and Transport Properties-REFPROP, Version 8.0, National Institute of Standards and Technology, Standard Reference Data Program, Gaithersburg, 2007.
- [90] D.E. Diller, M.J. Ball, Shear viscosity coefficients of compressed gaseous and liquid carbon dioxide at temperatures between 220 and 320 K and at pressures to 30 MPa, *Int. J. Thermophys.* 6 (1985) 619–629, <http://dx.doi.org/10.1007/BF00500334>.
- [91] V.N. Chukanov, V.P. Skripov, Spezifische Volumina vom überhitzten Wasser, *Teplofiz. Vys. Temp.* 9 (1971) 739–745.
- [92] G.S. Bamberger, G. Maurer, High-pressure (vapor+liquid) equilibrium in binary mixtures of (carbon dioxide+water or acetic acid) at temperatures from 313 to 353 K, *J. Supercrit. Fluid.* 17 (2000) 97–110, [http://dx.doi.org/10.1016/S0896-8446\(99\)00054-6](http://dx.doi.org/10.1016/S0896-8446(99)00054-6).
- [93] A. Valtz, A. Chapoy, C. Coquelet, P. Paricaud, D. Richon, Vapour-liquid equilibria in the carbon dioxide-water system, measurement and modelling from 278.2 to 318.2 K, *Fluid Phase Equilibr.* 226 (2004) 333–344, <http://dx.doi.org/10.1016/j.fluid.2004.10.013>.
- [94] H. Shu-Xin, C.M. Geoffrey, J.P.M. Trusler, Measurement and modeling of the phase behavior of the (carbon dioxide+water) mixture at temperatures from 298.15K to 448.15K, *J. Supercrit. Fluid.* 73 (2013) 87–96, <http://dx.doi.org/10.1016/j.supflu.2012.11.011>.
- [95] J.A. Briones, J.C. Mullins, M.C. Thies, B.U. Kim, Ternary phase equilibria for acetic acid-water mixtures with supercritical carbon dioxide, *Fluid Phase Equilibr.* 36 (1987) 235, [http://dx.doi.org/10.1016/0378-3812\(87\)85026-4](http://dx.doi.org/10.1016/0378-3812(87)85026-4).
- [96] G. Mueller, E. Bender, G. Maurer, Ber. Bunsen-Ges. Phys. Chem. 92 (1988) 148.
- [97] T. Sako, T. Sugeta, N. Nakazawa, T. Okubo, M. Sato, T. Taguchi, T.J. Hiaki, Phase equilibrium study of extraction and concentration of furfural produced in reactor using supercritical carbon dioxide, *J. Chem. Eng. Jpn.* 24 (1991) 449–455, <http://dx.doi.org/10.1252/jcej.24.449>.
- [98] Z. Cai, Z. Wu, Measurement and correlation of vapor-liquid equilibrium with CO<sub>2</sub> systems at high pressure, *Huaxue Gongcheng.* 24 (1996) 71–73.
- [99] S. Takenouchi, G.C. Kennedy, The binary system H<sub>2</sub>O–CO<sub>2</sub> at high temperatures and pressures, *Am. J. Sci.* 262 (1964) 1055–1074, <http://dx.doi.org/10.2475/ajs.262.9.1055>.
- [100] A. Hebach, A. Oberhof, N. Dahmen, Density of Water + Carbon Dioxide at Elevated Pressures: Measurements and Correlation, *J. Chem. Eng. Data* 49 (2004) 950–953, <http://dx.doi.org/10.1021/je034260i>.
- [101] F. Tabasinejad, Y. Barzin, R.G. Moore, S.A. Mehta, K.C. Van Fraassen, J. Rushing, K.E. Newsham, Water/ CO<sub>2</sub> System At High Pressure And Temperature Conditions: Measurement And Modeling Of Density In Equilibrium Liquid And Vapor Phases, January 1, Society of Petroleum Engineers, 2010, <http://dx.doi.org/10.2118/131636-MS>.
- [102] H. Teng, A. Yamasaki, M.K. Chun, H.J. Lee, Solubility of liquid CO<sub>2</sub> in water at temperatures from 278 K to 293 K and pressures from 6.44 MPa to 29.49 MPa and densities of the corresponding aqueous solutions, *Chem. Thermodyn.* 29 (1997) 1301–1310, <http://dx.doi.org/10.1006/jcht.1997.0249>.
- [103] R. Yaginuma, Y. Sato, D. Kodama, H. Tanaka, M. Kato, Saturated densities of carbon dioxide+Water mixture at 304.1 K and pressures to 10 MPa, *Nihon Enerugi Gakkaishi.* 79 (2000) 144–146.
- [104] J.A. Nighswander, N. Kalogerakis, A.K. Mehrotra, Solubilities of carbon dioxide in water and 1 wt. % sodium chloride solution at pressures up to 10 MPa and temperatures from 80 to 200° C, *J. Chem. Eng. Data* 34 (1989) 355–360, <http://dx.doi.org/10.1021/je00057a027>.
- [105] E.C. Efika, R. Hoballah, X. Li, E.F. May, M. Nania, Y. Sanchez-Vicente, J.P.M. Trusler, Saturated phase densities of (CO<sub>2</sub> + H<sub>2</sub>O) at temperatures from (293 to 450) K and pressures up to 64 MPa, *J. Chem. Thermodyn.* 93 (2016) 347–359, <http://dx.doi.org/10.1016/j.jct.2015.06.034>.
- [106] L.M.C. Pereira, A. Chapoy, R. Burgass, M.B. Oliveira, J.A.P. Coutinho, B.J. Tohidi, Study of the impact of high temperatures and pressures on the equilibrium densities and interfacial tension of the carbon dioxide/water system, *Chem. Thermodyn.* 93 (2016) 404–415, <http://dx.doi.org/10.1016/j.jct.2015.05.005>.
- [107] S.N. Joung, C.W. Yoo, H.Y. Shin, S.Y. Kim, K.P. Yoo, C.S. Lee, W.S. Huh, Measurements and correlation of high-pressure VLE of binary CO<sub>2</sub>-alcohol systems (methanol, ethanol, 2-methoxyethanol and 2-ethoxyethanol), *Fluid Phase Equilibr.* 185 (2001) 219–230, [http://dx.doi.org/10.1016/S0378-3812\(01\)00472-1](http://dx.doi.org/10.1016/S0378-3812(01)00472-1).
- [108] L.A. Galicia-Luna, A. Ortega-Rodriguez, D.J. Richon, New apparatus for the fast determination of high-pressure vapor-liquid equilibria of mixtures and of accurate critical pressures, *J. Chem. Eng. Data* 45 (2000) 265–271, <http://dx.doi.org/10.1021/je990187d>.
- [109] J.S. Lim, Y.Y. Lee, H.S. Chun, Phase equilibria for carbon dioxide-ethanol-water system at elevated pressures, *J. Supercrit. Fluids* 7 (1994) 219, [http://dx.doi.org/10.1016/0896-8446\(94\)90009-4](http://dx.doi.org/10.1016/0896-8446(94)90009-4).
- [110] S. Takishima, K. Saiki, K. Arai, S. Saito, Phase equilibria for the carbon dioxide-ethanol-water system, *J. Chem. Eng. Jpn.* 19 (1986) 48, <http://dx.doi.org/10.1252/jcej.19.48>.
- [111] Y.S. Feng, X.Y. Du, C.F. Li, Y.J. Hou, *Int. Symp. Supercrit. Fluids.* 75 (1988).
- [112] K. Nagahama, J. Suzuki, T. Suzuki, *Int. Symp. Supercrit. Fluids.* 143 (1988).
- [113] K. Suzuki, H. Sue, M. Itou, R.L. Smith, H. Inomata, K. Arai, S.J. Saito, Isothermal vapor-liquid equilibrium data for binary systems at high pressures: carbon dioxide-methanol, carbon dioxide-ethanol, carbon dioxide-1-propanol, methane-ethanol, methane-1-propanol, ethane-ethanol, and ethane-1-propanol systems, *Ind. Eng. Chem. Chem. Eng. Data Ser.* 35 (1990) 63–66, <http://dx.doi.org/10.1021/je00059a020>.
- [114] D.W. Jennings, R.J. Lee, A.S. Teja, Vapor-liquid equilibria in the carbon dioxide + ethanol and carbon dioxide + 1-butanol systems, *J. Chem. Eng. Data* 36 (1991) 303–307, <http://dx.doi.org/10.1021/je00003a013>.
- [115] J.H. Yoon, H.S. Lee, H. Lee, High-pressure vapor-liquid equilibria for carbon dioxide + methanol, carbon dioxide + ethanol, and carbon dioxide + methanol + ethanol, *J. Chem. Eng. Data* 38 (1993) 53–55, <http://dx.doi.org/10.1021/je00009a012>.
- [116] H. Tanaka, M. Kato, Vapor-liquid equilibrium properties of carbon dioxide + ethanol mixture at high pressures, *J. Chem. Eng. Jpn.* 28 (1995) 263–266, <http://dx.doi.org/10.1252/jcej.28.263>.
- [117] D. Chan-Yih, C.J. Chiehming, C. Chiu-Yang, Phase equilibrium of ethanol + CO<sub>2</sub> and acetone + CO<sub>2</sub> at elevated pressures, *J. Chem. Eng. Data* 41 (1996) 839–843, <http://dx.doi.org/10.1021/je960049d>.
- [118] C.J. Chang, C.Y. Day, C.M. Ko, K.L. Chiu, Densities and P-x-y diagrams for carbon dioxide dissolution in methanol, ethanol, and acetone mixtures, *Fluid Phase Equilibr.* 131 (1997) 243, [http://dx.doi.org/10.1016/S0378-3812\(96\)03208-6](http://dx.doi.org/10.1016/S0378-3812(96)03208-6).
- [119] N. Zhang, X. Zheng, Vapor-liquid equilibria for carbon dioxide-ethanol and carbon dioxide-iso-Propanol system, *Huaxue Gongcheng.* 25 (1997) 51–56.
- [120] C.J. Chang, K.L. Chiu, C.Y. Day, A new apparatus for the determination of P-x-y diagrams and Henry's constants in high pressure alcohols with critical carbon dioxide, *J. Supercrit. Fluids* 12 (1998) 223–237, [http://dx.doi.org/10.1016/S0896-8446\(98\)00076-X](http://dx.doi.org/10.1016/S0896-8446(98)00076-X).
- [121] J.L.Mendoza de la Cruz, L.A. Galicia-Luna, *Int. Electron. J. Physico. Chem. Data* 5 (1999) 157–164.
- [122] H.J. Chen, H.Y. Chang, E.T.S. Huang, T.C. Huang, A new phase behavior apparatus for supercritical fluid extraction study, *Ind. Eng. Chem. Res.* 39 (2000) 4849–4852, <http://dx.doi.org/10.1021/ie000099i>.
- [123] M.M. Elbaccouch, M.B. Raymond, J.R. Elliott, High-pressure vapor-liquid equilibrium for R-22 + ethanol and R-22 + ethanol + water, *J. Chem. Eng. Data* 45 (2000) 280–287, <http://dx.doi.org/10.1021/je990136g>.
- [124] Y.L. Tian, M. Han, L. Chen, J. Feng, Y. Qin, Study on vapor-liquid phase equilibria for CO<sub>2</sub>-C<sub>2</sub>H<sub>5</sub>OH system, *Wuli Huaxue Xuebao.* 17 (2001) 155–160.
- [125] O. Elizalde-Solis, L.A. Galicia-Luna, Solubility of thiopene in carbon dioxide and carbon dioxide + 1-propanol mixtures at temperatures from 313 to 363K, *Fluid Phase Equilibr.* 230 (2005) 51–57, <http://dx.doi.org/10.1016/j.fluid.2004.11.018>.
- [126] D. Kodama, M.J. Kato, High-pressure phase equilibrium for carbon dioxide + ethanol at 291.15 K, *Ind. Eng. Chem. Chem. Eng. Data Ser.* 50 (2005) 16–17, <http://dx.doi.org/10.1021/je034243t>.
- [127] Z. Knez, M. Skerget, L. Ilic, C.J. Lutge, Vapor liquid equilibrium of binary CO<sub>2</sub> organic solvent systems (ethanol, tetrahydrofuran, ortho-xylene,

- meta-xylene, para-xylene), *J. Supercrit. Fluids* 43 (2008) 383–389, <http://dx.doi.org/10.1016/j.supflu.2007.07.020>.
- [128] Y. Maeta, M. Ota, Y. Sato, R.L. Smith Jr, H. Inomata, Measurements of vapor–liquid equilibrium in both binary carbon dioxide–ethanol and ternary carbon dioxide–ethanol–water systems with a newly developed flow-type apparatus, *Fluid Phase Equilib.* 405 (2015) 96–100, <http://dx.doi.org/10.1016/j.fluid.2015.07.025>.
- [129] M. Kariznovi, H. Nourozieh, J. Abedi, Experimental measurements and predictions of density, viscosity, and carbon dioxide solubility in methanol, ethanol, and 1-propanol, *J. Chem. Thermodyn.* 57 (2013) 408–415, <http://dx.doi.org/10.1016/j.jct.2012.10.002>.
- [130] M. Stievano, N. Elvassore, High-pressure density and vapor liquid equilibrium for the binary systems carbon dioxide ethanol, carbon dioxide acetone and carbon dioxide dichloromethane, *J. Supercrit. Fluids* 33 (2005) 7–14, <http://dx.doi.org/10.1016/j.supflu.2004.04.003>.
- [131] D. Kodama, M. Kato, High-pressure phase equilibrium for carbon dioxide + ethanol at 291.15 K, *J. Chem. Eng. Data* 50 (2005) 16–17, <http://dx.doi.org/10.1021/je034243t>.
- [132] B. Seifried, F. Temelli, Density of carbon dioxide expanded ethanol at (313.2, 328.2, and 343.2) K, *J. Chem. Eng. Data* 55 (2010) 2410–2415, <http://dx.doi.org/10.1021/je900830s>.
- [133] I. Tsivintzelis, D. Missopolinou, K. Kalogiannis, C. Panayiotou, Phase compositions and saturated densities for the binary systems of carbon dioxide with ethanol and dichloromethane, *Fluid Phase Equilib.* 224 (2004) 89–96, <http://dx.doi.org/10.1016/j.fluid.2004.06.046>.
- [134] L.C. Baker, T.F. Anderson, Some phase relationships in the three-component liquid system carbon dioxide + water + ethanol at high pressures, *J. Am. Chem. Soc.* 79 (1957) 2071, <http://dx.doi.org/10.1021/ja01566a013>.
- [135] G.S. Gurdial, N.R. Foster, S.L.J. Yun, K.D. Tilly, Phase behavior of supercritical fluid–entrainer systems, *ACS Symp. Ser.* 514 (1993) 34–45.
- [136] L.A. Galicia-Luna, A. Ortega-Rodriguez, D. Richon, New apparatus for the fast determination of high pressure vapor–liquid equilibria of mixtures and of accurate critical pressures, *J. Chem. Eng. Data* 45 (2000) 265–271, <http://dx.doi.org/10.1021/je990187d>.
- [137] S.D. Yeo, S.J. Park, J.W. Kim, J.C. Kim, Critical Properties of Carbon Dioxide + Methanol, + Ethanol, + 1-Propanol, + 1-Butanol, *J. Chem. Eng. Data* 45 (2000) 932–935, <http://dx.doi.org/10.1021/je000104p>.
- [138] S.N. Joung, C.W. Yoo, H.Y. Shin, S.Y. Kim, K.P. Yoo, C.S. Lee, W.S. Huh, *Fluid Phase Equilib.* 185 (2001) 219–230, [http://dx.doi.org/10.1016/S0378-3812\(01\)00472-1](http://dx.doi.org/10.1016/S0378-3812(01)00472-1).
- [139] M. Sun, R. Ye, T. Liu, H. Liu, Measurements of the critical temperature and pressure of ethylene + benzene + ethylbenzene mixture, *Chin. J. Chem. Eng.* 10 (4) (2002) 469 <https://www.cheric.org/research/tech/periodicals/view.php?seq=385575>.
- [140] H. Zhu, Y.L. Tian, L. Chen, J. Feng, H. Fu, Studies on Vapor-liquid Phase Equilibria for SCF CO<sub>2</sub>+CH<sub>3</sub>OH and SCF CO<sub>2</sub>+C<sub>2</sub>H<sub>5</sub>OH Systems, *Gaodeng Xuexiao Huaxue Xuebao.* 23 (2002) 1588–1591.
- [141] W. Wu, J. Ke, M. Poliakoff, Phase boundaries of CO<sub>2</sub> + toluene, CO<sub>2</sub> + acetone, and CO<sub>2</sub> + ethanol at high temperatures and high pressures, *J. Chem. Eng. Data* 51 (2006) 1398–1403, <http://dx.doi.org/10.1021/je060099a>.
- [142] S. Sima, V. Feriou, D. Geana, New high pressure vapor liquid equilibrium and density predictions for the carbon dioxide + ethanol system, *J. Chem. Eng. Data* 56 (2011) 5052–5059, <http://dx.doi.org/10.1021/je2008186>.
- [143] Y. Sun, Y. Li, J. Zhou, R. Zhu, Y. Tian, Experimental determination and calculation of the critical curves for the binary systems of CO<sub>2</sub> containing ketone, alkane, ester and alcohol, respectively, *Fluid Phase Equilib.* 307 (2011) 72–77, <http://dx.doi.org/10.1016/j.fluid.2011.05.005>.
- [144] L. Gil, S.T. Blanco, C. Rivas, E. Laga, J. Fernandez, M. Artal, I. Velasco, Experimental determination of the critical loci for {n-C<sub>6</sub>H<sub>14</sub> or CO<sub>2</sub> + alkan-1-ol} mixtures. Evaluation of their critical and subcritical behavior using PC-SAFT EoS, *J. Supercrit. Fluids* 71 (2012) 26–44, <http://dx.doi.org/10.1016/j.supflu.2012.07.008>.
- [145] G.M. Kontogeorgis, I.V. Yakoumis, H. Meijer, E. Hendriks, T. Moorwood, Multicomponent phase equilibrium calculations for water–methanol–alkane mixtures, *Fluid Phase Equilibria.* 158–160 (1999) 201–209, [http://dx.doi.org/10.1016/S0378-3812\(99\)00060-6](http://dx.doi.org/10.1016/S0378-3812(99)00060-6).
- [146] M.G. Bjørner, G.M. Kontogeorgis, Modeling derivative properties and binary mixtures with CO<sub>2</sub> using the CPA and the quadrupolar CPA equations of state, *Fluid Phase Equilib.* 408 (2016) 151–169, <http://dx.doi.org/10.1016/j.fluid.2015.08.011>.
- [147] Design Institute for Physical Properties, DIPPR DIADEM Database, Version 10.0, Brigham Young University, Provo (Utah), USA, (n.d.).
- [148] L. Mingjian, M. Peisheng, X. Shuqian, A modification of a in SRK equation of state and vapor–liquid equilibria prediction, *Chin. J. Chem. Eng.* 15 (2007) 102–109, [http://dx.doi.org/10.1016/S1004-9541\(07\)60041-X](http://dx.doi.org/10.1016/S1004-9541(07)60041-X).
- [149] W.R. Ji, D.A. Lempe, Density improvement of the SRK equation of state, *Fluid Phase Equilib.* 130 (1997) 49–63, [http://dx.doi.org/10.1016/S0378-3812\(96\)03190-1](http://dx.doi.org/10.1016/S0378-3812(96)03190-1).
- [150] A.M. Palma, M.B. Oliveira, A.J. Queimada, J.A.P. Coutinho, Re-evaluating the CPA EoS for improving critical points and derivative properties description, *Fluid Phase Equilib.* 436 (2017) 85–97, <http://dx.doi.org/10.1016/j.fluid.2017.01.002>.
- [151] A.P.C.M. Vinhal, W. Yan, G.M. Kontogeorgis, Evaluation of equations of state for simultaneous representation of phase equilibrium and critical phenomena, *Fluid Phase Equilib.* 437 (2017) 140–154, <http://dx.doi.org/10.1016/j.fluid.2017.01.011>.